Universidade de Aveiro
Departamento de
Eletrónica, Telecomunicações e Informática
2017

Gonçalo
Amorim Dias

Antenas 3D para utilização em Transmissão de Energia sem Fios

3D Antennas for Wireless Power Transmission

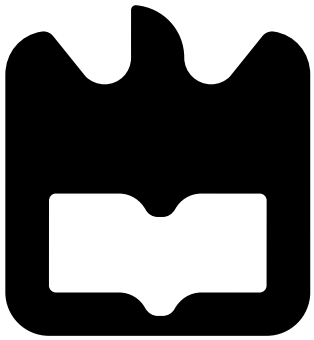

Gonçalo
Amorim Dias

Antenas 3D para utilização em Transmissão de Energia sem Fios

3D Antennas for Wireless Power Transmission

Dissertação apresentada à Universidade de Aveiro para cumprimento dos requesitos necessários à obtenção do grau de Mestre em Engenharia Eletrónica e Telecomunicações, realizada sob a orientação científica de Nuno Borges de Carvalho, Professor Catedrático do Departamento de Eletrónica, Telecomunicações e Informática da Universidade de Aveiro, sob co-orientação científica do Doutor Pedro Renato Tavares de Pinho, Professor Adjunto da Área Departamental de Engenharia Eletrónica e Telecomunicações e de Computadores do Instituto Superior de Engenharia de Lisboa.

o júri / the jury

presidente / president

Doutor José Carlos Esteves Duarte Pedro
Professor Catedrático da Universidade de Aveiro (por delegação da Reitora da Universidade de Aveiro)

vogais / examiners committee

Doutor Nuno Miguel Gonçalves Borges de Carvalho
Professor Catedrático da Universidade de Aveiro (orientador)

Doutor Luís Manuel de Sousa Pessoa
Investigador Sénior do Instituto de Engenharia de Sistemas e Computadores do Porto

“The transmission of power without wires will very soon create an industrial revolution and such as the world has never seen before”

— Nikola Tesla, 1906, letter to George Westinghouse

“Learn from yesterday, live for today, hope for tomorrow. The important thing is not to stop questioning. ”

— Albert Einstein

agradecimentos / acknowledgements

Em primeiro lugar quero deixar um especial agradecimento aos meus pais e à minha irmã. Agradecer por todo o esforço e apoio que me deram. Sem eles não conseguiria alcançar este percurso académico de que me tanto orgulho.

Tal como eles, quero também agradecer aos meus avós, aos meus tios, às minhas primas, aos meus padrinhos, à Ana e à família dela que me ajudaram em todo o meu percurso académico, pelo apoio e por sempre acreditarem que era capaz de aqui chegar.

Aos meus amigos, que me proporcionaram bons momentos. Com todas as aventuras, brincadeiras e acima de tudo boa disposição.

Aos meus orientadores, pela orientação prestada nesta minha primeira abordagem à investigação académica.

À equipa técnica do Instituto de Telecomunicações que se mostrou sempre disponível para ajudar.

Palavras-Chave Antenas 3D, Lentes, Transmissão de Potência Sem Fios, Antenas Microstrip

Resumo

A impressão em 3D tem assistido a um crescimento bastante acentuado nos últimos cinco anos, especialmente desde que começaram a aparecer soluções deste tipo de tecnologia a preços muito mais baixos e para o utilizador comum.

A liberdade de desenho associada às estruturas tridimensionais permite criar geometrias complexas que produzem características de radiação muito específicas para aplicações bastante exigentes. E, hoje em dia é possível fazer isto sem precisar de grandes orçamentos. Nesta dissertação é explorada a solução baseada em lentes, através da tecnologia de impressão 3D.

São apresentadas três antenas, uma antena microstrip alimentada por acoplamento sem lente, a segunda com uma lente semiesférica estendida e a terceira com uma lente esférica. O objetivo destas antenas é fornecer ou captar potência para redes de sensores passivos no espaço. As antenas apresentadas funcionam na banda K, mais concretamente a 20 GHz. A estas frequências as lentes tornam-se aceitáveis em tamanho para muitas aplicações.

Com esta dissertação concluiu-se que a utilização de lentes impressas em impressoras 3D é uma solução interessante para aumentar o ganho e focar o campo eletromagnético de uma antena. Estas características permitem criar antenas pequenas e compactas com um ganho elevado e que conseguem ter uma performance semelhante a outras de maior custo e dimensões, como por exemplo, as parabólicas, agregados, ou cornetas.

Keywords 3D Antennas, Lens, Wireless Power Transmission, Microstrip Antennas

Abstract

The 3D printing has seen a very strong growth in the last five years, especially since began to appear solutions of this kind of technology at much lower prices and for common user.

The design of freedom associated with the three-dimensional structures can create complex geometries that produce very specific characteristics of radiation for very demanding applications. Today, it is possible to do this without big budgets. In this dissertation the lens based solution is explored through 3D printing technology.

Three antennas are presented, one microstrip coupled antenna without lens, the second with an extended hemispherical lens and the third with a spherical lens. The purpose of these antennas is to provide or capture power for passive sensor networks in space. These antennas operate in the K band, more specifically at 20 GHz. In these frequencies, the lenses become acceptable in size for many applications.

With this dissertation it was concluded that the use of printed lenses in 3D printers is an interesting solution to increase the gain and to focus the electromagnetic field of an antenna. These characteristics allow to create small and compact antennas with a high gain that can perform a similar performance to others with higher cost and dimensions, such as reflectors, arrays, or horn antennas.

Contents

List of Figures

List of Tables

Acronyms

3D	Three Dimensional
AC	Alternate Current
ACES	Applied Computational Electromagnetics Society
CAD	Computer Aided Designed
CST	Computer Simulation Technology
DC	Direct Current
DLA	Dieletric Lens Antenna
DMB	Digital Multimedia Broadcasting
EM	Electromagnetic
FDM	Fused Deposition Modeling
FFF	Fused Filament Fabrication
FNBW	First Null Beamwidth
GSM	Global System for Mobile Communications
HF	High Frequency
HPBW	Half Power Beam Width
IoT	Internet of Everything
IoT	Internet of Things
LTE	Long Term Evolution
PLA	Polylactic Acid
RF	Radio frequency
RFID	Radio Frequency Identification
UMTS	Universal Mobile Telecommunication System
URSI	International Union for Radio Science
VSWR	Voltage Standing Wave Ratio
WPT	Wireless Power Transmission
WSN	Wireless Sensor Network

Chapter 1

Introduction

1.1 Motivation

The three dimensional (3D) printing has seen a very strong growth in the last five years, especially since began to appear solutions of this kind of technology at much lower prices and for common user.

It is possible to exploit the technology to create antennas with more complex shapes and in three dimensions quickly and much cheaper, befor here only accessible to development teams of high budget projects, such as military or space.

Electronic devices have almost become a basic need given that the majority of jobs today depend on it to be done. Greater investment in research regarding the Internet of Things (IoT) is still forcing us to a larger dependency on self-sufficient electronic systems.

The greatest disadvantage of current electronic devices comes from their dependence of external power connections or batteries in order to operate. It is therefore necessary to make these devices capable to be powered on a more efficient and versatile manner.

The advancement of wireless power transmission (WPT) systems gets us more like a really wireless world, as it was envisioned by Nikola Tesla and William C. Brown in the past century.

This will empower society a more agreeable utilization of gadgets, be it from the integration of these mechanisms in implantable medical devices, the use of backscattering on sensors, easier charge of electronic devices, the power could be transmitted to the places where the wired transmission is not possible [1] .

1.2 Objectives

The core objective of this master of science dissertation is to design, build and test aperture coupled microstrip antennas for WPT with a dielectric lens made on a 3D printer. It should work properly in the frequency around 20 GHz, have an input impedance of 50 Ω and be highly directive.

The objective of these antennas is for transmission or harvesting energy at 20 GHz frequency in space applications, for example, to be used as a transmitting source to power up passive sensors in space.

1.3 Dissertation Outline

Including this introductory chapter, this dissertation is divided into five chapters. In this first chapter an introduction to the dissertation work was presented, along with the motivation, objectives and original contributions. Chapter two and three, serve to contextualize WPT and basic theoretical concepts required for design the proposed antennas, while chapter four present the design and simulation of three antennas. In chapter five some conclusions are presented and possible future directions of this work is also discussed.

More specifically, chapter two presents the basics and fundamentals concepts of antennas. This chapter focus on two types of antenna: microstrip patch antennas and lens antenna.

Chapter three explains how WPT works and presents some techniques to improve the efficiency of rf-to-dc converters used for WPT, few examples are also presented.

Chapter four introduces the overall characteristics of the aperture coupled microstrip antenna with dielectric lens. First is presented a design and simulation of microstrip aperture coupled antenna without lens, then the same antenna, but with extended hemispherical lens. In this second antenna the building process and measured results are also presented.

Finally a third antenna design is presented, this antenna presents a solution for the problems detected in the previous antenna. The solution is based in spherical lens. At the end of this chapter is presented a comparison between simulated and measured results, also a performance analysis between the two 3D antennas and three commercial antennas.

Then, in chapter five, summarizes the work done and main conclusions drawn, presenting suggestions for some future work possibilities based on the work developed so far.

1.4 Original Contributions

This dissertation has lead to the writing of scientific papers that were submitted to two separate conferences.

- The first, Gonçalo Dias, Pedro Pinho and Ricardo Gonçalves, Nuno Carvalho, "3D Antenna for Wireless Power Transmission", was accepted to compete for the Best Student Paper Award at the 10 th Congress of the Portuguese Committee of the International Union for Radio Science (URSI) - "Comunicações em cenários de segurança e emergência". This article is presented in Appendix B.

- The remaining article, Gonçalo Dias, Pedro Pinho and Ricardo Gonçalves, Nuno Carvalho, "3D Antenna for Wireless Power Transmission" (see Appendix C), was submitted for the 2017 International Applied Computational Electromagnetics Society (ACES) Symposium. This article is presented in Appendix C.

In the course of this work were produced two antennas with high directive radiation pattern and with small dimensions. These characteristics are ideal for WPT, because it's possible to maximize the transmitted/received power in one direction and it's easy to integrate these antennas in a portable device.

Although this dissertation is directed to WPT, these antennas can also be used for communications.

Chapter 2

Wireless Power Transmission

The possibility to transfer energy from one place to another without cables is not new. This idea appears in the nineteenth century with Nikola Tesla and more later in 1960 by William C. Brown.

In nowadays we have already many applications that make use of WPT, for example RF identification (RFID) and inductive charge for mobile phones. This examples use different technologies to transfer power. RFID use RF microwaves to power and read RFID tags.

The inductive charging uses inductive power coupling, that take advantage from coupling effect between two coils to transfer power. This technology permits to transfer higher power levels than RFID, but is more limited in terms of maximum distance between transmitter and receiver, normally is a few centimeters. A lot of WPT examples are shown in [11].

In this dissertation is explored the solution based on RF microwaves to WPT. Two antennas are proposed with high directive radiation pattern, this give the ability to focus the power in one direction.

The advancements in ultra low power semiconductors and the requirements of IoT, smart cities and machine-to-machine communications are pushing forward the development in WPT solutions.

2.1 Energy Harvesting (Radio Frequency) and Wireless Sensor Network (WSN)

Energy harvesters take power from ambient sources present around us, this can be wind, solar, vibration, electromagnetic (EM), thermoelectric, radio frequency and acoustic.

This dissertation focus is on the WPT technique using the EM energy specifically RF, but only propose a solution for the antenna side. The RF sources in this case could be GSM, UMTS, LTE, Wifi, radio stations, all RF signals can power the harvester.

The power collected by RF energy harvesting techniques is usually less than few milliwatt, but some devices only need a few μA to operate, as stated in [3].

A great factor contributing for energy harvesting research and development is the advancements in ultra-low-power components.

A typical WPT system is presented in Figure 2.1. In the left side we have the transmitting antennas that can be dedicated for WPT or not, the harvester or sensor can collect power from existing sources, like the ones presented in the figure. On right side is shown a possible solution for a harvester device or a wireless sensor.

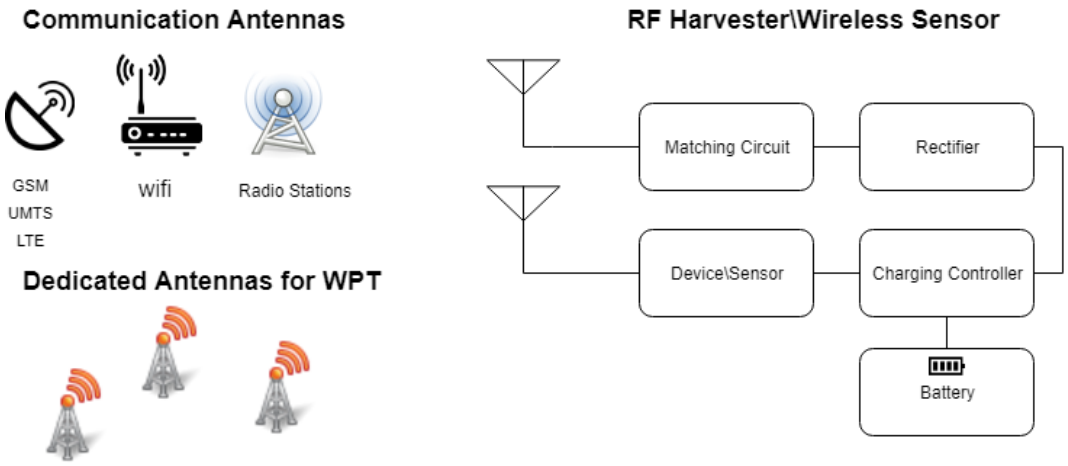

Figure 2.1: Wireless Power System Architecture

The RF signals are captured by a multiband antenna or single antenna depended on application, also could be omnidiretional or directive. In this dissertation high directive antenna is presented with more detail in next chapters.

The matching circuit is used to capture the maximum power at required frequency range. The design of this circuit take into account the antenna impedance and the impedance of the circuit that receives alternate current (AC) signal typically a rectifier and voltage multiplier. The matching circuit could be eliminated if the antenna have impedance matched with the circuit.

The RF is AC signal, to get a DC signal out of the AC signal, a rectifier circuit is employed, by employing multiple stages the required output voltage can be obtained. The voltage output is twice the input peak voltage minus twice the diode threshold voltage, for this reason a Schottky diode is an ideal component for RF energy harvesting because offer low forward voltage and high switching speed.

The number of voltage doubler stages can boost the input AC voltages to a higher level and convert it to the DC, but as the Figure 2.2 shows with more stages the efficiency start to decrease. Trade-off between efficiency and output voltage have to take into account to the RF to DC design. Another technique to improve the efficiency is to use multi-sine signals or using chaotic waveforms to transmitting power [4] [5].

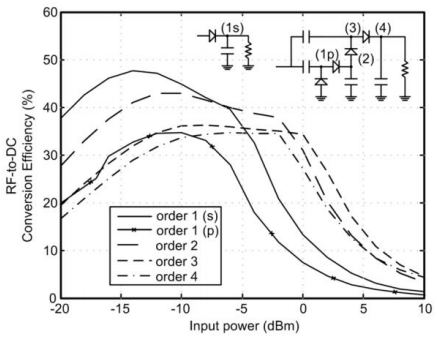

Figure 2.2: RF to DC converter efficiency and typical circuit [6]

Wireless sensor networks are formed by many of this devices that can communicate and take power by an external RF source that could be a base station or an mobile station. For example, imagine a farmer wants to know the state of their plantations. He puts on the soil this devices that measured the humidity, temperature and level of fertilizer. Then he send a drone that have an RF source to power and communicate with the sensors. If he want to do this with traditional sensor he had to spent a lot of money on copper lines only for power this devices. This is only a possible solution of many that WSN will bring when this technology is fully matured. Recently advances in backscattering communications, like in [13] and [14], show that we are getting closer to this brilliant future.

Chapter 3

Antennas

An antenna, by definition in [15], is "that part of a transmitting or receiving system that is designed to radiate or to receive electromagnetic waves". This device gives the ability to transfer (EM waves) energy/information wirelessly, dependent on the application.

The basic operation of transmitting and receiving antennas is shown in Figure 3.1.

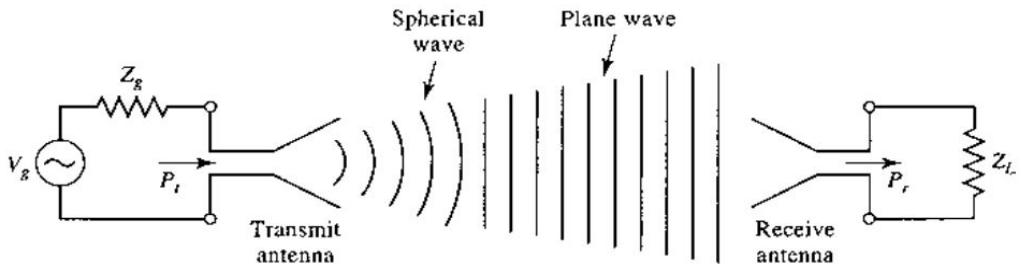

Figure 3.1: Basic operation of transmitting and receiving antennas [16]

From circuit analysis theory an RF transmitter can be seen was a Thevenin source that delivers energy to the transmitting antenna. This antenna converts an EM wave on a transmission line into a plane wave that propagates in free space.

The receiving antenna catch part of the incident plane wave and delivery into a load-/impedance, that can be any circuit of an specif application (communication or WPT system).

3.1 Fundamental Basic Parameters of Antennas

This section introduce the essential and important parameters of an antenna from the circuit point of view and the field point of view. Definitions of various parameters are necessary to describe the performance of an antenna. Some of the parameters are interrelated and not all of them need be specified for complete description of the antenna performance. All these definitions and equations were taken from [15] [16] [17] [18].

Field Regions

The antenna field can be divided into three regions: reactive near-field, radiating near-field (Fresnel) and far-field (Fraunhofer) regions as shown in Figure 3.2 and is conditions in Table 3.1, [17] :

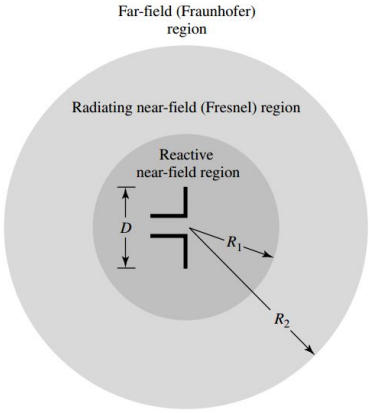

Figure 3.2: Field regions of an antenna [17]

Antenna size = D	$\boldsymbol{D << \lambda}$	$\boldsymbol{D \approx \lambda}$	$\boldsymbol{D >> \lambda}$
Reactive near field	$r < \lambda/2\pi$	$r < \lambda/2\pi$	$r < \lambda/2\pi$
Radiating near field	$\lambda/2\pi < r < 3\lambda$	$\lambda/2\pi < r < 3\lambda$ and $2D^2/\lambda$	$\lambda/2\pi < r < 2D^2/\lambda$
Far field	$r > 3\lambda$	$r > 3\lambda$ and $2D^2/\lambda$	$r > 2D^2/\lambda$

Table 3.1: Near-field and far-field conditions [17]

Radiation Pattern

Radiation pattern, is defined in [15], as "the spatial distribution of a quantity that characterizes the electromagnetic field generated by an antenna ". The radiation pattern is obtained in the far-field region and is represented in directional coordinates. Power pattern is usually plotted on a logarithmic scale and sometimes is normalized to their maximum value.

There are three main categories of radiation patterns (Figure 3.3):

- *Isotropic*, equal radiation in all directions. This only a concept reference antenna.
- *Omnidirectional*, equal radiation around a plane.
- *Directional*, main lobe of radiation pointing points into a single direction.

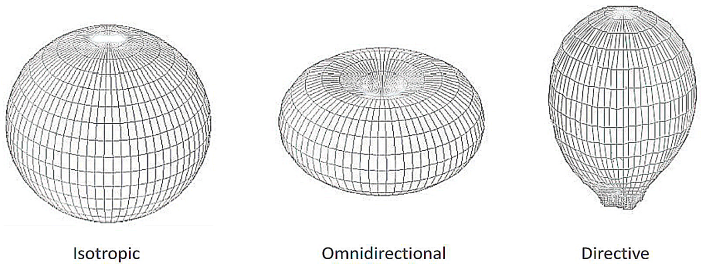

Figure 3.3: Principal antenna patterns

Analyzing the radiation pattern it's possible to take a "whole picture" about the radiation characteristics. The most common usually to characterize the radiation pattern are shown bellow and can be analyzed with more detail in [15] [18].

- *Half-Power Beamwidth* (HPBW) is used to quantify how sharp is the beam;
- *First Null Beamwidth* (FNBW) is also used to quantify how sharp is the beam;;
- *First side-lobe level* if this value is to small, for example -30 dB, show the antenna have a good directivity at the main lobe;
- *Front-to-back ratio* another way to identify the directivity of the antenna;
- *Null positions* used for anti-interference and positioning.

Directivity

It is defined in [15], as "the ratio of the radiation intensity in a given direction from the antenna to the radiation intensity averaged over all directions ". In mathematical form, it can be written as:

$$D = \frac{4\pi U}{P_{rad}} \tag{3.1}$$

Where P_{rad} is the total radiated power and U is the radiation intensity.

Gain and Radiation Efficiency of Antennas

The gain of an antenna is defined in [15] as "the ratio of the radiation intensity, in a given direction, to the radiation intensity that would be obtained produced if the power accepted by the antenna were isotropically radiated". Mathematically, the gain can be written as:

$$G = \frac{4\pi U}{P_{in}} \tag{3.2}$$

Where U is again the radiation intensity and P_{in} is the total input power accepted by the antenna.

The radiation efficiency, is defined in [15] as "the ratio of the total power radiated by an antenna to the net power accepted by the antenna from the connected transmitter".

Input Impedance and Radiation Resistance

Antenna input impedance (Z_a) is defined in [17] as "the impedance presented by an antenna at its terminals or the ratio of the voltage to current at its terminals". Mathematically, the input impedance is:

$$Z_a = \frac{V_{in}}{I_{in}} = R_a + jX_a \tag{3.3}$$

The input impedance is a complex number and the real part consists of two components: the radiation resistance and the loss resistance of the antenna.

Reflection Coefficient, Return Loss and VSWR

When we design an antenna an important factor to take into account is the adaption to a given operational frequency. The parameters that quantify this adaption are the reflection coefficient, return loss and voltage standing wave ratio (VSWR). According to [17], these three parameters are related as the equations bellow shown :

- reflection coefficient (a complex number):

$$\Gamma = \frac{Z_a - Z_0}{Z_a + Z_0} \tag{3.4}$$

- return loss (expressed in dB):

$$L_{RT} = -20Log_{10}(|\Gamma|) \tag{3.5}$$

- VSWR (a ratio between 1 and infinity):

$$VSWR = \frac{1 + |\Gamma|}{1 - |\Gamma|} \tag{3.6}$$

The commonly required specification of an antenna is $L_{RT} > 10dB$ or $VSWR < 2$.

Types of Antennas

There are many types of antennas. They are summarized and grouped in categories on Figure 3.4:

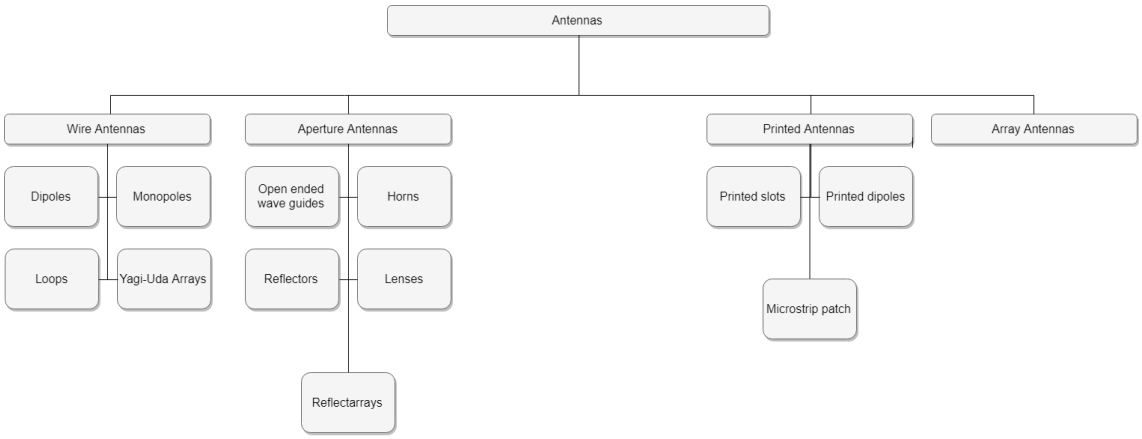

Figure 3.4: Antennas types

The antennas can also be grouped by criteria. In figure 3.5 are present the most commonly criteria:

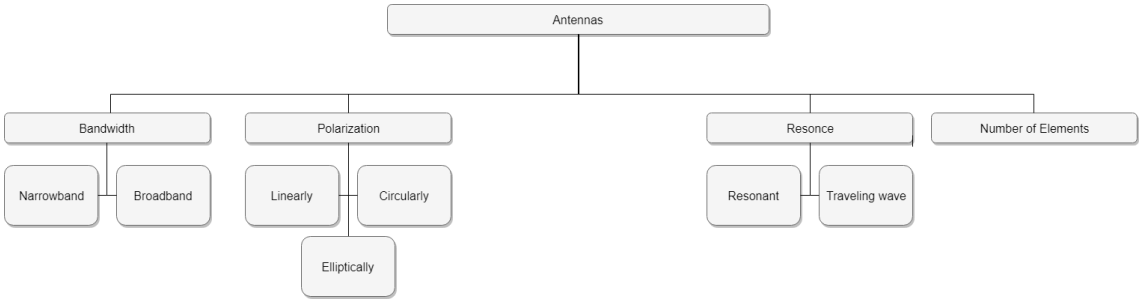

Figure 3.5: Antennas grouped by criteria

3.2 Microstrip Patch Antennas

The geometry of an microstrip antenna is shown in Figure 3.6. This type of antenna is widely used in nowadays, like in mobile phones. The advantage of this configuration are the easy integration in printed circuits and the versatility, for example, it's possible to tune the resonant frequency of the antenna by changing the patch length. This versatility is very useful when we are designed an antenna on an EM simulator and it is possible to parameterize the antenna.

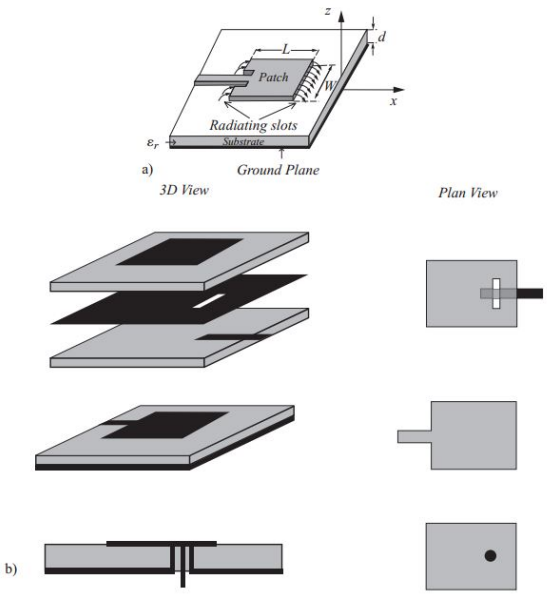

Figure 3.6: Microstrip antennas and their feeds (a) a microstrip antenna with its coordinates; (b) three feeding configurations: coupling feed, microstrip feed and coaxial feed [17]

This antenna can be fed by a microstrip line, a coaxial line or by coupling. All three are viable ways depending on application to be used. In this dissertation the coupling method was chosen, because for higher frequencies it's more easy to tune the antenna by changing the slot length and the gap size on the ground plane. The shape of the patch can be any form depending of the required radiation pattern, polarization and resonant frequency.

Its shown in [17] that the length and width of the rectangular patch is given by:

$$L = \frac{1}{2f_r\sqrt{\epsilon_{reff}}\sqrt{\epsilon_0\mu_0}} - 2\Delta L \tag{3.7}$$

Where ΔL is the enlargement on L, this effect is also explained with more detail in[17], is given by:

$$\Delta L = 0.412d\left(\epsilon_{reff} + 0.3\right)\left(W/d + 0.264\right) / \left[\left(\epsilon_{reff} - 0.258\right)\left(W/d + 0.8\right)\right] \tag{3.8}$$

Patch width is given by:

$$W = \frac{1}{2f_r\sqrt{\epsilon_0\mu_0}}\sqrt{2/(\epsilon_r + 1)} \tag{3.9}$$

It's possible to see from 3.7, 3.8 and 3.9 equations that for higher frequencies the size of the patch decreases. If the square patch is desired the only thing to do is kept the patch width with the same dimension of the length of the patch.

Microstrip Line

To design the feed line of an microstrip coupled antenna, the microstrip line transmission equations must be taken into account. The microstrip line configuration is very similar to

microstip antenna. This line is composed by a printed conductor of width W on thin substrate of thickness d and relative permittivity ϵ_r. Figure 3.7 show this configuration:

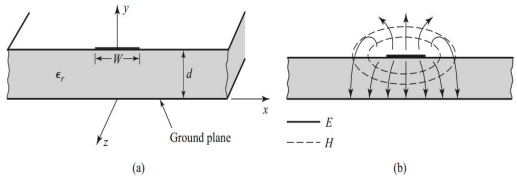

Figure 3.7: Microstrip transmission line. (a) Geometry. (b) Electric and magnetic field lines [16]

The impedance of this transmission has been widely studied and according to [16] and [17] the best approximation is:

$$Z_0 = \begin{cases} \frac{60}{\sqrt{\epsilon_{reff}}} ln\left(\frac{8d}{W} + \frac{W}{4d}\right), & \text{for } W/d \leq 1 \\ \\ \frac{120\pi}{\sqrt{\epsilon_{reff}}[W/d+1.393+0.667ln(W/d+1.444)]}, & \text{for } W/d \geq 1 \end{cases} \tag{3.10}$$

The effective dielectric constant, ϵ_{reff}, of a microstrip line is approximately:

$$\epsilon_{reff} = \frac{\epsilon_r + 1}{2} + \frac{\epsilon_r - 1}{2} \frac{1}{\sqrt{1 + 12d/W}} \tag{3.11}$$

Analyzing the equations 3.10 and 3.11, if the substrate thickness and relative permittivity are maintained, the greater width of the line, smaller the impedance of the same, the opposite also occurs when smaller width of the line, greater the impedance of the same.

Know the relative permittivity and loss tangent of the substrate are essential when a EM simulator is used to optimized the microstrip lines and antennas. This values change with the frequency of operation. If a wrong value is used on simulation this can make that the simulated values diverge with the measured ones. There are some methods to measure this proprieties of the material, there is a good discussing of this techniques in [19], [20], [21], [22] and [23]. On table 3.2 some common material used on antenna substrates with their respective relative permittivity and loss tangent.

	ϵ_r	tan δ
Alumina	9.8	0.0004
$LaAlO_3$	24	0.0001
MgO	9.8	0.00001
Quartz (SiO_2)	3.8	0.0004
Sapphire (Al_2O_3)	9.4 and 10.8	0.00002
Epoxy (FR4)	4.43 @1GHz	0.01
FR2 (flame resistant 2)	4.50 @1MHz	0.025
GaAs	13	0.0006
LCP	3.1	0.002
PTFE (Teflon)	2.1	0.0004
PTFE-glass	2.1–2.55	0.001
PTFE-ceramic	10.2	0.002
RT/Duroid 5870	2.33	0.0012
RT/Duroid 5880	2.22	0.0009
RT/Duroid 6002, 6202	2.94	0.0012
RT/Duroid 6006	6.15	0.0019
RT/Duroid 6010	10.2	0.0023

Table 3.2: Some common substrates for a microstrip [17]

3.3 Lens Antenna

The millimeter-wave and sub-millimeter frequency bands are very attractive for various modern indoor and outdoor applications. At these frequencies lenses become acceptable in size and weight for many applications. Lens antennas consist of two main parts: the feeding antenna that can be any other type of antenna (horns, dipoles, microstrip (patch) antennas, and even arrays of antenna elements) and lens that collimate incident divergent energy to prevent it from spreading in undesired directions.

Integrated dielectric lens antennas (DLAs) are widely used in various communication, radar, and imaging systems in the millimeter (mm) and sub-mm wave bands. The principal components of such antennas are dielectric lenses used for correction of radiation patterns of primary feeds, like horn or printed antennas.

Additionally, improvement of radiation efficiency is achieved due to a better matching (for the waveguide feeds) and a suppression of the surface waves (for the substrate mounted antennas). The common demands to novel DLAs are compact size and specific radiation patterns. A desired compromise between these two characteristics is not always easily achievable. Preliminary computer aided design (CAD) enables one to minimize the time and cost of a prototype development.

There are primarily two different lens designs used for realizing different goals. Canonical (hyperbolical, bihyperbolical, elliptical, hemispherical) or shaped lens antennas are used for collimating the radiated energy, or, in case of shaped designs, for shaping the beam to required radiation patterns, while circular-cylindrical and spherical lenses are mostly used for beam scanning with single or multiple feed possibility [24] [25] [26].

Chapter 4

Aperture Coupled Microstrip Antenna with Dielectric Lens

4.1 Basics

Aperture-coupled feed was originally proposed by Pozar [27]. This configuration consists of two substrates separated by a ground plane. On the bottom side of the lower substrate, there is a microstrip feed line which has the form of an open-circuit stub while the top side of the upper substrate contains the microstrip patch element. The energy is electromagnetically coupled from the feed line to the patch through a slot in the ground plane as shown in Figure 4.1.

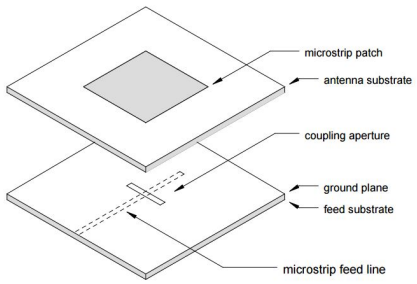

Figure 4.1: Geometry of the basic aperture coupled microstrip antenna [28]

There principal advantage of coupling feed is that the feed network and the patch are well isolated and the surface wave excitation can be better controlled by select different substrate materials, like the ones shown in Table 3.2, for the feed and radiating elements. The disadvantage of this feeding is the back radiation level from the feed network, but can be minimized by tunning correctly the slot size.

4.2 Design Parameters

The design of an aperture-coupled feed for a patch antenna configuration involves the careful selection of several parameters. Know how this parameters affects the antenna behavior is essential, when we have an parameterized antenna in a EM simulator and we want to

tune a specif characteristics, like input impedance and resonant frequency, for example.

This parametric study already was been made by Pozar in [28], bellow is shown a Table 4.1 that resumes and compiles his conclusions and were confirmed when i was tuning the presented antennas in the next sections.

Design parameter	**Effect in antenna behviour**
Antenna substrate dielectric constant	Bandwidth and radiation efficiency, with lower permittivity leads to wider impedance bandwidth and reduced surface wave excitation.
Antenna substrate thickness	Bandwidth and coupling level. A thicker substrate leads to wider bandwidth, but less coupling for a given aperture size.
Feed line position relative to slot	For maximum coupling, the feed line should be positioned at right angles to the center of the slot. Moving the feed line from the slot will reduce the coupling.
Feed line width	Impose the characteristic impedance of the feed line, and affects the coupling to the slot.
Feed substrate dielectric constant	Should be selected for good microstrip circuit qualities.
Feed substrate thickness	Thinner leads to less spurious radiation from feed lines, but higher loss.
Length of tuning stub	Tune the excess reactance of the slot.
Microstrip patch length	Impose the resonant frequency of the antenna.
Microstrip patch width	Tune the resonant resistance of the patch, wider leads to a lower resistance, like microstrip lines.
Position of the patch relative to the slot	Maximum coupling occurs when the patch is centered over the slot. Moving the patch relative to the slot in the H-plane direction has little effect, while moving the patch relative to the slot in the E-plane (resonant) direction will decrease the coupling level.
Slot length	Tune the coupling and the back radiation level. The slot should be made no larger than is required for impedance matching.
Slot width	Tune the coupling level, but to a much less degree than the slot width.

Table 4.1: Design Parameters and its effects in antenna performance [28]

4.3 Design and Simulation

In order to get acquainted with the software tools for this project, a first attempt was made to design an aperture coupled microstrip antenna without dielectric lens, that could work at 20 GHz and has an input impedance of 50 Ω.

In order to do so, an appropriate substrate must be selected. In this case, the choice was based on the material availability, so that prototypes could be produced without much more expense.

The selected substrate was Isola Astra MT [29], with dielectric (ϵ_r) of 3 and tangent loss (δ) of 0.0018. For the antenna substrate was used 1.52 mm height and for feed substrate 0.76

mm .

For simulation purposes, the selected conductor was an infinitely thin copper padding with a conductivity of $5.8 \times 10^7 S/m$.

The aperture coupled patch antenna is modeled in Computer Simulation Technology (CST). Simulation results are used as the baseline antenna performance for comparison against all parametric adjustments.

Figure 4.2 shows the antenna layers and nominal dimensions in millimeters, all this values were calculated from the equations in previous chapter 2 and tunned by simulation.

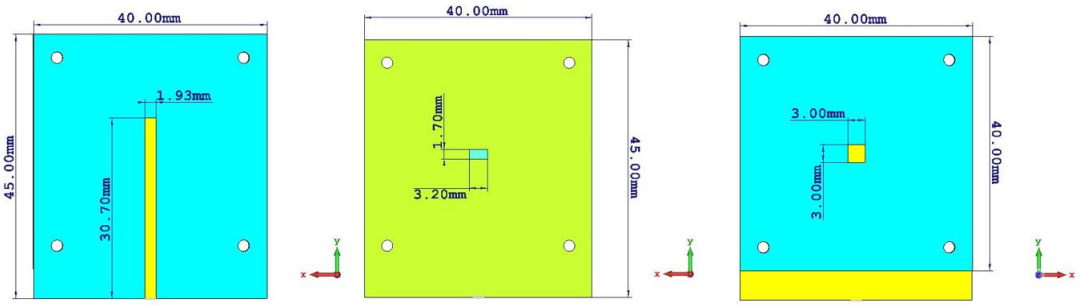

Figure 4.2: Simulated aperture-coupled microstrip patch antenna

The iterative antenna design optimization, in Figure 4.3, is carried out as follows: The network parameters and radiation pattern are calculated with an initial design equations. After this an error Δ is calculated quantifying the difference between the simulated/measured and goals parameters. If the error is below a certain limit, the optimization is terminated, otherwise the antenna parameters are disturbed by means of an optimization and the new network parameters and the deviation from the measurement is calculated. The last steps are repeated until the desired accuracy is reached.

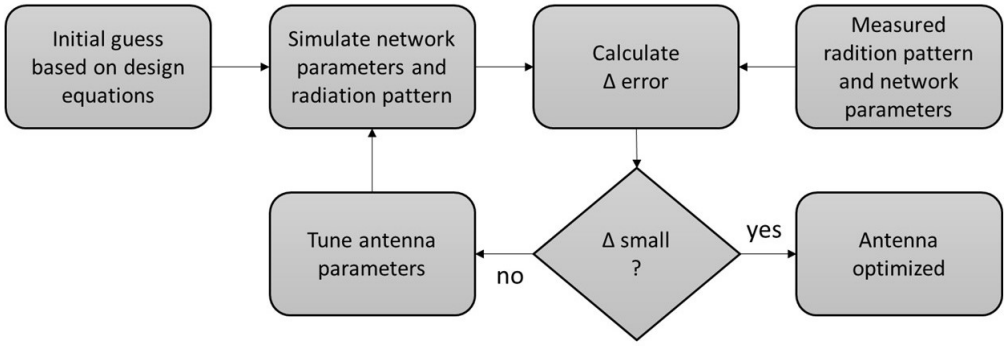

Figure 4.3: Sketch of the iterative antenna design optimization

The center frequency, input impedance, bandwidth, and radiation patterns are determined and summarized below.

The return loss present in Figure 4.4 can clarify that the obtained bandwidth is around 2.15 GHz and show the resonating frequency of the antenna is 20 GHz.

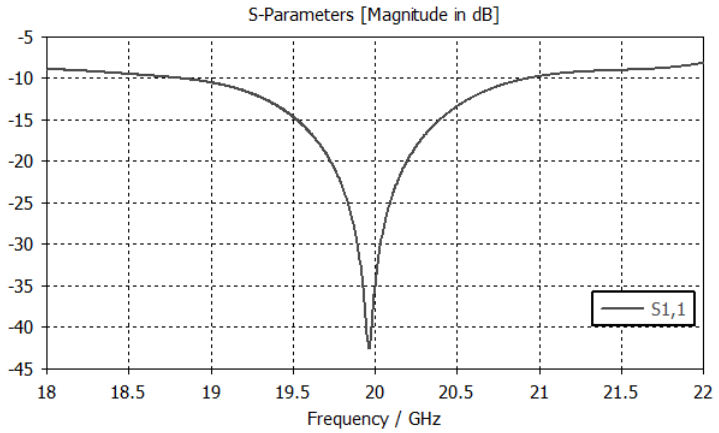

Figure 4.4: Simulated return loss of the aperture-coupled microstrip patch antenna

From Figure 4.5 it's possible to see that the input impedance at 20 GHz is around 50 ohms, how it was designed.

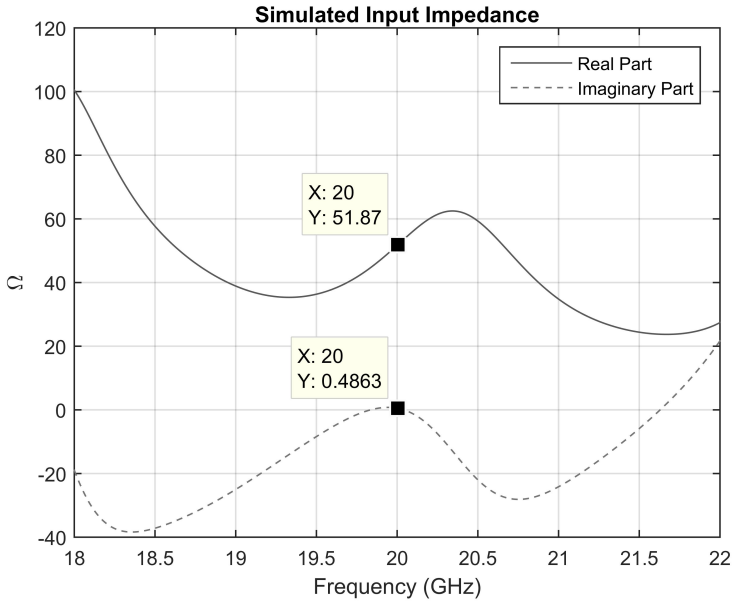

Figure 4.5: Simulated input impedance of the aperture-coupled microstrip patch antenna

As expected, the antenna presents in Figure 4.6 a semi-spherical radiation pattern and low gain (6 dBi). In general the antenna meets initial objectives, the next step is design a lens to shape the radiation pattern and making it high directive. This study is presented in next section.

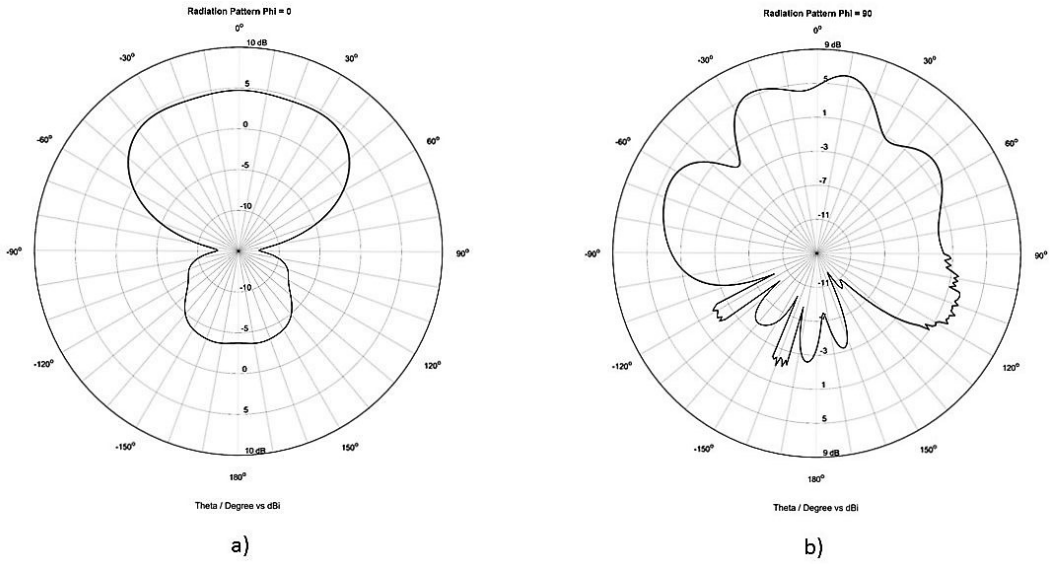

Figure 4.6: Simulated radiation pattern of the aperture-coupled microstrip patch antenna. (a) Phi=0, (b) Phi=90.

4.4 Extended hemispherical lens fed by an aperture-coupled microstrip patch antenna

4.4.1 Design and Simulation

The proposed 3D antenna is presented in Figure 4.7. As the previous model, this was build in an Isola Astra MT [29] substrate.

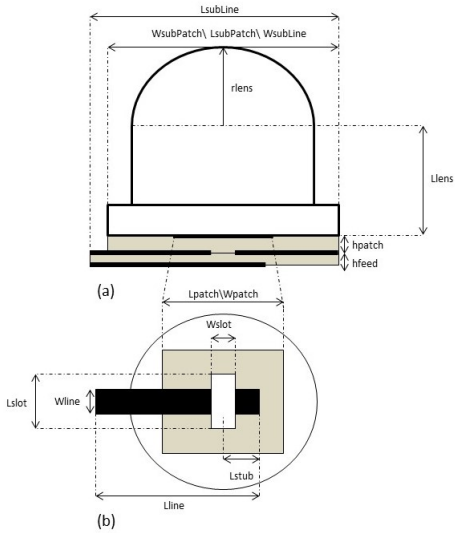

Figure 4.7: Extended hemispherical lens fed by an aperture-coupled microstrip patch antenna (a) Cross-section view and (b) top view

From the design analysis, the proposed antenna is a square patch microstrip coupled, with a extended hemispherical lens.

This geometry was chosen and adapted, in order to allow the highest gain and directivity possible, for a 3D printed small antenna. The microstrip coupled antenna size is 40x45x(1.52+0.76) mm^3 and the lens 40x40x55 mm^3.

The lens is used to focus the beam of lower gain feed antenna to produced highly directive pattern with low side lobe levels. The radiating microstrip patch element is etched on the top of the antenna substrate, and the microstrip feed line is etched on the bottom of the feed substrate like in Figure 4.1.

The lens "shift" the center frequency, so it's necessary make some tuning at the antenna parameters with a compromise to the radiation pattern, gain and input impedance. The lens is fabricated with polylactic acid (PLA) that has an estimated relative permittivity of 1.8 and a loss tangent of 0.01 [30]. The values obtained after simulation and optimization are shown in Table 4.2.

Parameter	**Value (mm)**	**Parameter**	**Value (mm)**
L_{patch}	3	Lens size	40x40x55
W_{patch}	3	L_{line}	25
L_{slot}	3.5	L_{stub}	5.5
W_{slot}	1.7	W_{line}	1.93
$L_{subPatch}$	40	h_{patch}	1.52
$W_{subPatch}$	40	h_{feed}	0.76
$L_{subLine}$	45	L_{lens}	35
$W_{subLine}$	40	r_{len}	20

Table 4.2: Design parameters of aperture-coupled microstrip patch antenna with extended hemispherical lens

One of the challenges of this kind of design is the impedance match of the antenna and specific radiation patterns. Therefore, after balancing this issue, which led to the values presented in the previous table, the simulated return loss and radiation pattern obtained for this antenna can be viewed in Figure 4.8 .

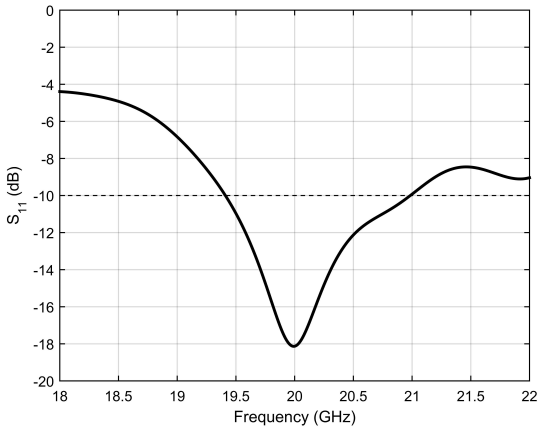

Figure 4.8: Simulated return loss of the 3D antenna

From the return loss graphic in Figure 4.8 it's seen that the resonating frequency is 20 GHz. The bandwidth of the antenna can be extracted from this parameter as the set of frequencies that satisfy the condition S11 < -10 dB. The bandwidth is from 19.41 to 20.98 GHz. The simulated input impedance at 20 GHz of this antenna was 53 + j12.5 Ω.

The radiation pattern of the aperture-coupled microstrip patch antenna with extended hemispherical lens has a directive characteristic.

The simulated radiation pattern is presented in Figure 4.9 and 4.10 . It presents a radiation efficiency of 92,4% and a high directivity at main lobe of 17 dBi. Analyzing the Figure 4.9 it's obvious that 3D lens focus the beam of lower gain feed antenna to produce a highly directive pattern. The antenna with lens has more 10.86 dB of gain than aperture-coupled microstrip patch antenna without 3D lens.

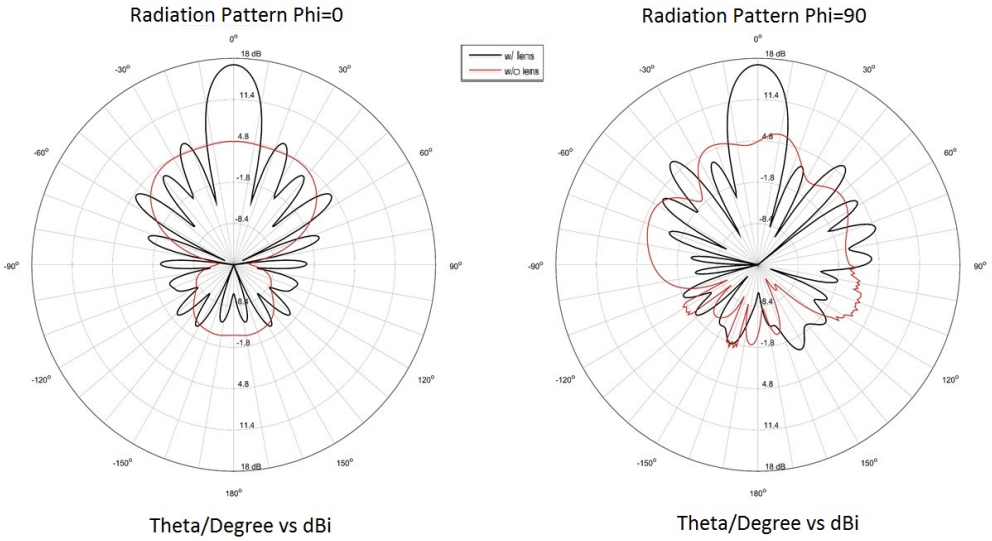

Figure 4.9: Simulated Radition Pattern of aperture-coupled microstip patch antenna with extended hemispherical lens

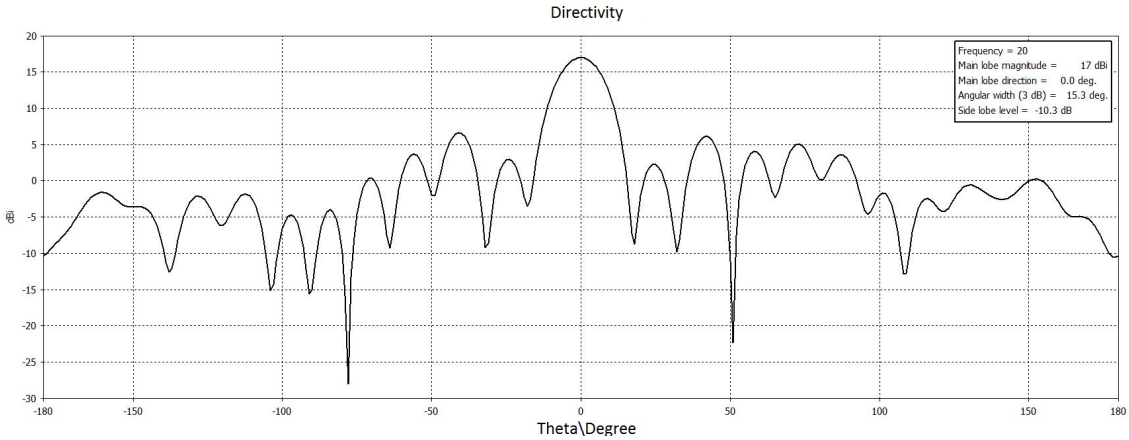

Figure 4.10: Simulated cartesian plot of far-field directivity

4.4.2 Real Antenna

For the construction of the lens was used a 3D printer that gives freedom of geometric forms and precision to make the designed model presented in previous section. The material used for printing was PLA. The software used to model the lens was OpenSCAD [31]. This tool is not an interactive modeller, instead it is something like a 3D-compiler that reads in a script file that describes the object and renders the 3D model from this script file, like Figure 4.11. This gives full control over the modelling process and enables easily change any step in the modelling process or make designs that are defined by configurable parameters.

```
1
2
3  union(){
4
5
6  // square base
7  difference(){
8
9      cube([40,40,5]);
10
11     translate([4,4,-1]){cylinder(10,1,1,$fn=50);}
12
13     translate([36,4,-1]){cylinder(10,1,1,$fn=50);}
14
15     translate([36,36,-1]){cylinder(10,1,1,$fn=50);}
16
17     translate([4,36,-1]){cylinder(10,1,1,$fn=50);}
18
19     };
20
21
22 // cylinder + sphere
23 translate([20,20,5]){cylinder(30,20,20,$fn=50);}
24
25 translate([20,20,35]){sphere(r = 20,$fn=50);}
26
27 }
```

Figure 4.11: Script used to generate the extended hemispherical lens

For the lens printing was used BEETHEFIRST[32] 3D printer and BEESOFT to control

and calibrate the 3D printer. The material used for the lens was PLA and 90% density printing with the previous presented dimensions. The prototyped 3D anntenna is present in Figure 4.12.

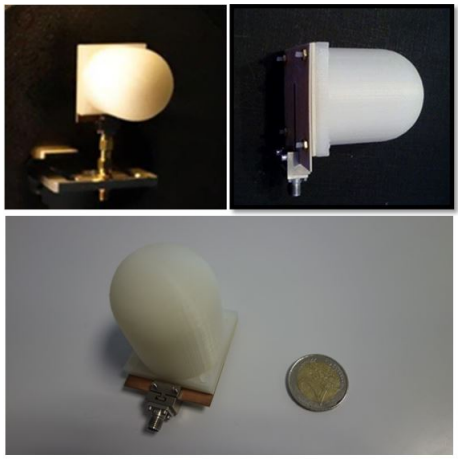

Figure 4.12: Prototyped 3D anntenna

The measured return loss is shown in Figure 4.13, in which one can compare the simulated with the measured results.

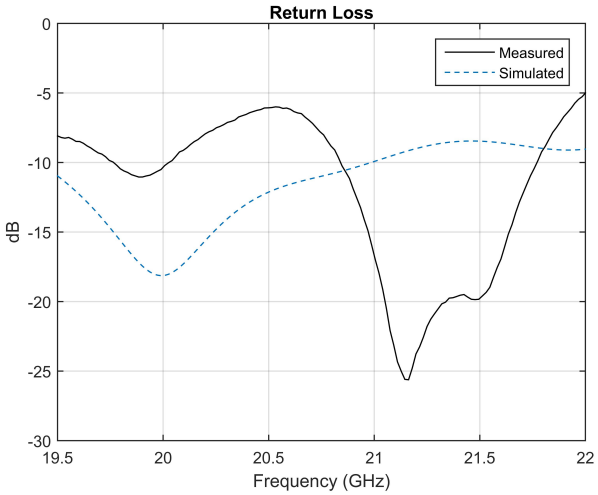

Figure 4.13: Simulated (Blue) and Measured (Black) return loss for the 3D antenna

The prototype shows some deviations regarding the operation frequencies, which might be due to a misalignment of the slot and patch stacked structure, and also due to an erroneous definition of the PLA dielectric values used for simulation. Still, the prototyped antenna shows a fairly good agreement with the simulated results. It has a bandwidth from 19.78 - 20.02 GHz and 20.85 - 21.76 GHz.

The resulting farfield can be seen in Figure 4.14. High directivity at the main beam can be achieved with DLA configuration. This proves that 3D lens focus the beam of lower gain feed antenna to produce a highly directive pattern. The disadvantage of this antenna is the

side lobe level is a little high, around -10 dB.

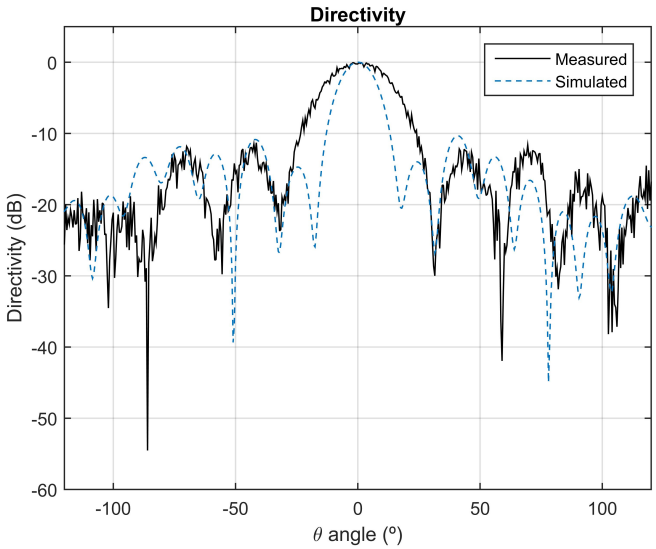

Figure 4.14: Simulated (Blue) and Measured (Black) directivity for the 3D antenna

4.5 Spherical lens fed by an aperture-coupled microstrip patch antenna

4.5.1 Design and Simulation

In order to get a better return loss and consequently better match at 20 GHz a spherical lens (Luneberg lens) was chosen, Figure 4.15. This lens contains a little air gap between the microstrip aperture coupled patch antenna and the lens.

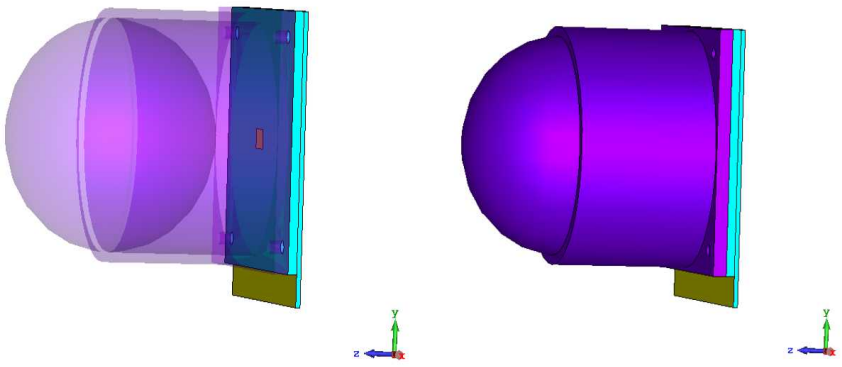

Figure 4.15: Spherical lens fed by an aperture-coupled microstrip patch antenna

The term Luneberg lens refers to a family of lenses with two axial focus. They can be both outside the lens or one inside and the other outside. The most useful case, however, is the lens with one focus on its surface, while the second one is at infinity. Thus, an axial point on the lens surface is focused to an axial point at infinity, on the opposite side of the lens.[33]

Once again this antenna was designed in an Isola Astra MT [29] substrate and the spherical lens in PLA. From the design analysis, the proposed antenna is a patch microstrip coupled with spherical lens.

The final design and dimensions obtained after simulation and optimization are shown in Figure 4.16.

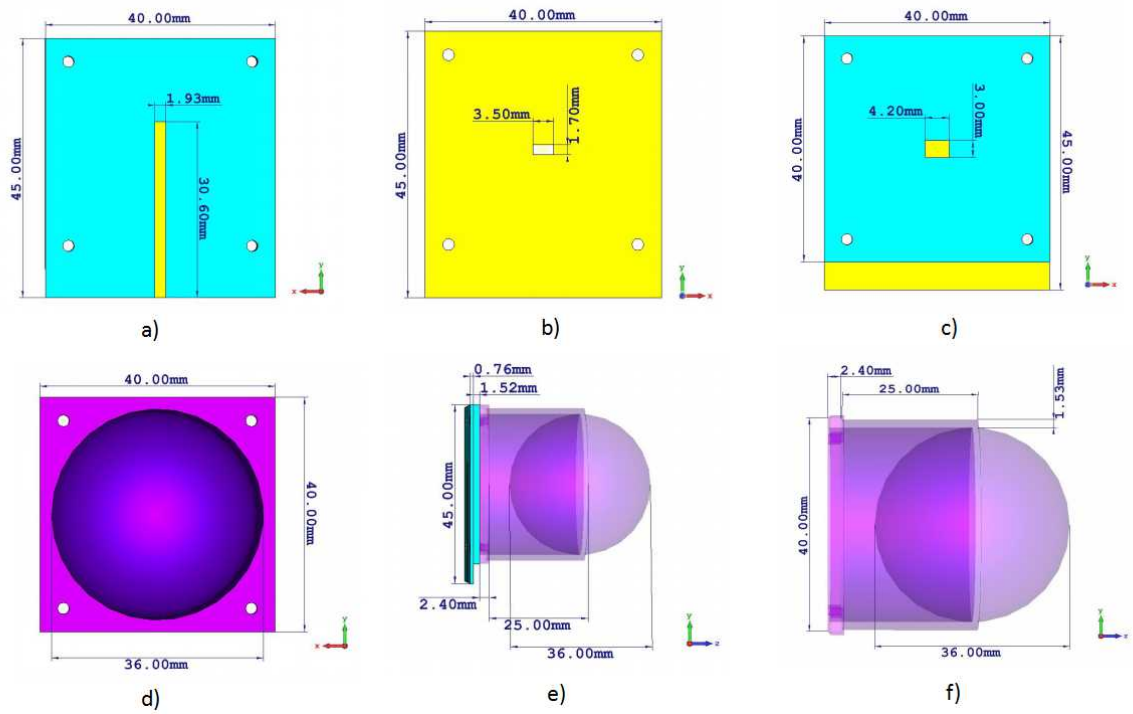

Figure 4.16: Spherical lens fed by an aperture-coupled microstrip patch antenna final design and dimensions. (a) Feed substrate, (b) Ground plane, (c) Patch substrate, (d) Bottom view spherical lens, (e) Side view antenna, (f) Side view spherical lens

The results from the simulation of this patch are plotted in Figure 4.17, presenting a return loss of -25,56 dB at 20 GHz and a bandwidth of 2 GHz.

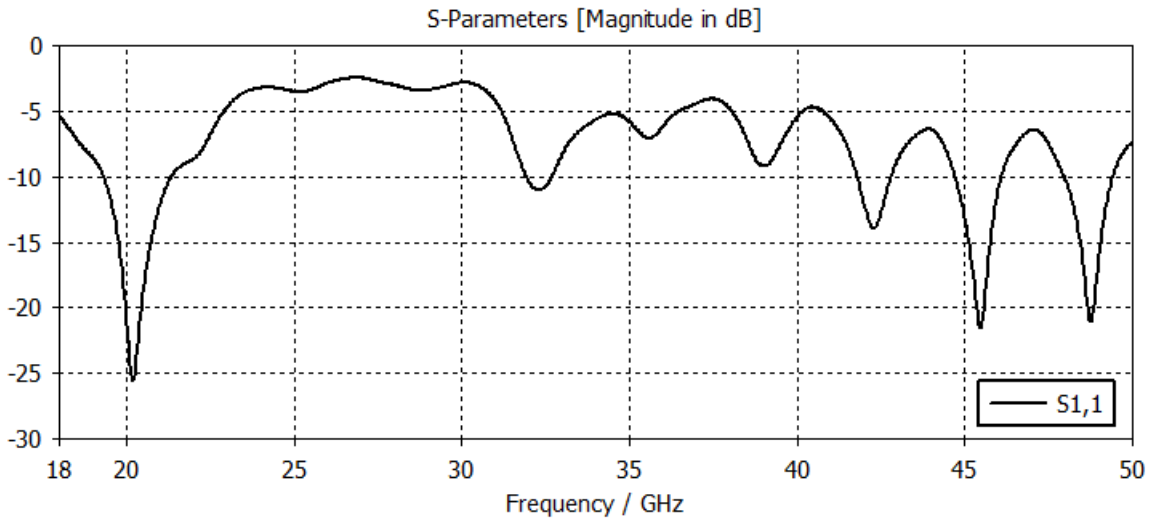

Figure 4.17: Simulated return loss of spherical lens fed by an aperture-coupled microstrip patch antenna

The impedance response simulated for this antenna is shown in Figure 4.18. The input impedance at 20 GHz is around 50 Ω, like the initial design requirement.

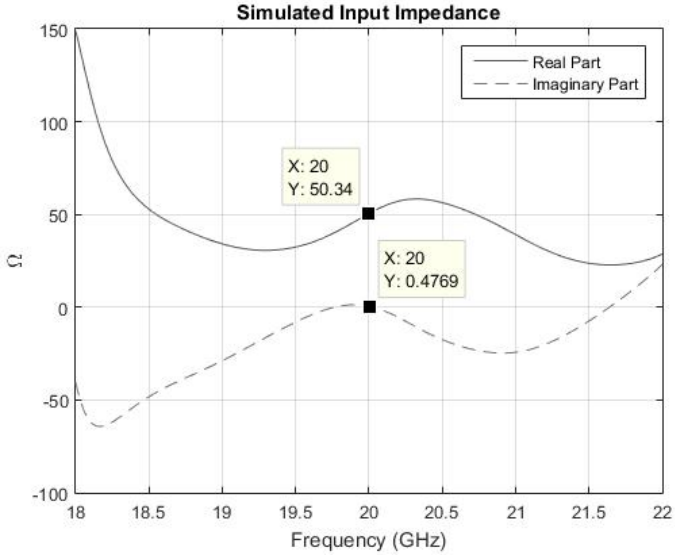

Figure 4.18: Simulated input impedance of spherical lens fed by an aperture-coupled microstrip patch antenna

Analyzing Figure 4.19 it's obvious the reduction of the side lobes level, but this improvement bring a slight decrease on gain and small increase of beamwidth. Nothing significant, given the improvements presented.

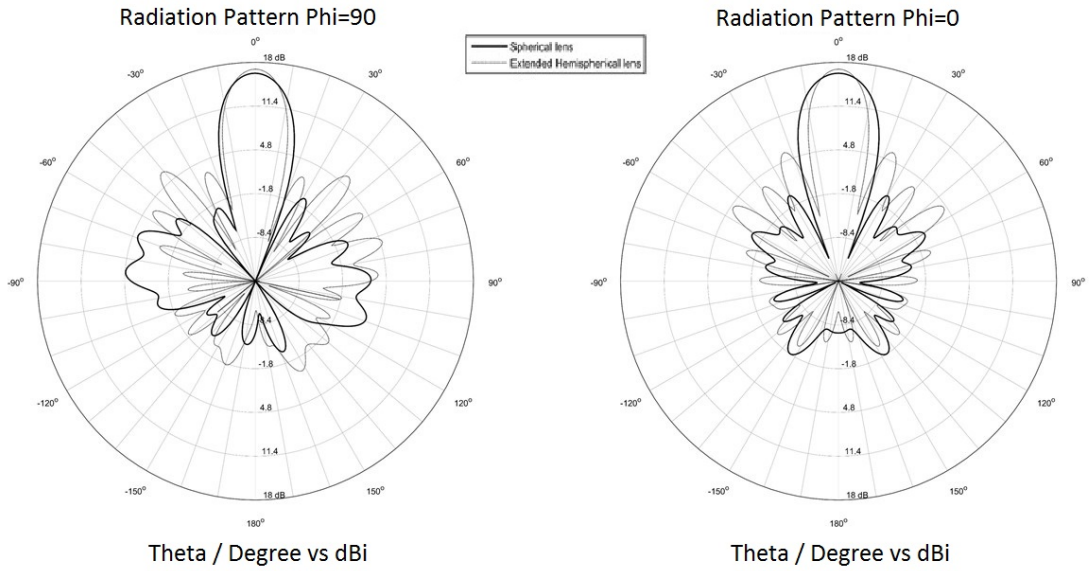

Figure 4.19: Simulated Radition Pattern of spherical lens fed by an aperture-coupled microstrip patch antenna

4.5.2 Real Antenna

For the construction of this antenna, the same material was used from the previous presented antenna, but this time a special focus was taken in the alignment of the gap in common ground plane with the patch. Built antenna is shown in Figure 4.20.

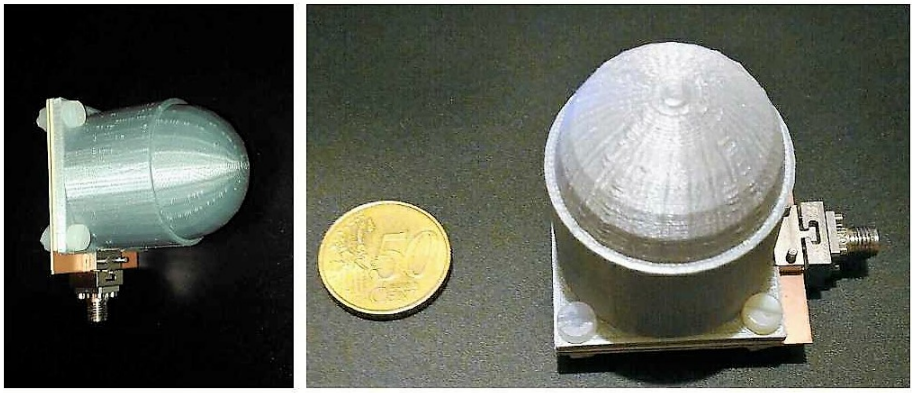

Figure 4.20: Prototyped 3D antenna

The comparison between simulated and measured return loss can be observed in Figure 4.21.

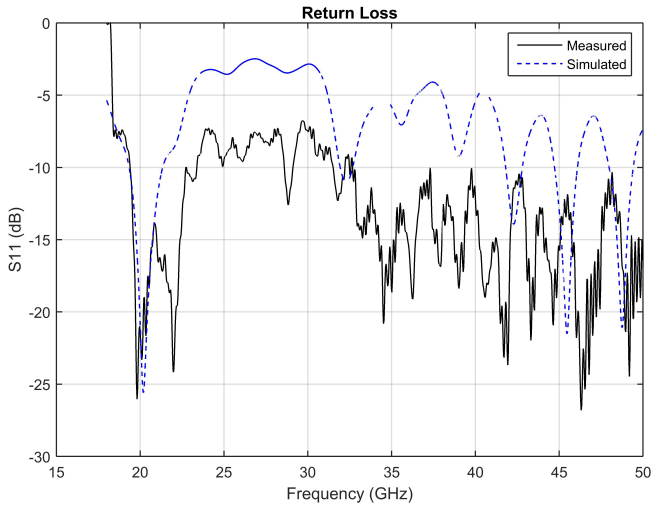

Figure 4.21: Simulated (Blue) and Measured (Black) return loss for the 3D antenna spherical lens

The prototyped spherical lens antenna shows a fairly good agreement with the simulated results. It has a bandwidth from 19.40-23.38 GHz.

Although the return loss simulated values are very close to the measured values, in the radiation pattern the same was not observed in Figure 4.22.

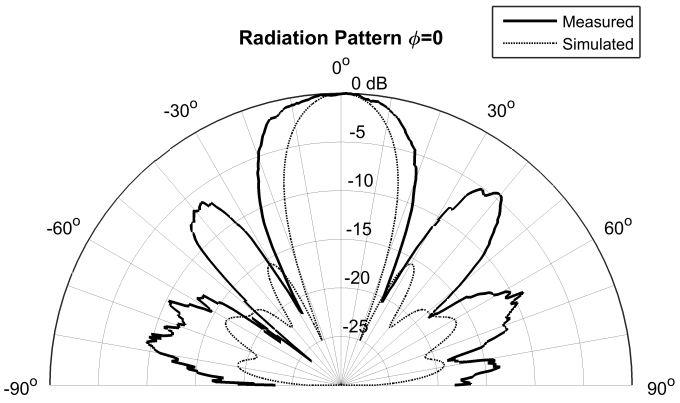

Figure 4.22: Simulated (Dashed) and Measured (Black) radiation pattern for the 3D antenna spherical lens

The effect of the spherical lens is visible, like in the previous the lens, they focus the beam of lower gain feed antenna to produce a highly directive pattern. The beamwidth achieved was 31.5° closed to the simulated value 21.5°. The main difference between the measured and simulated values are the side lobe level, in the measured result the side lobe level is higher than the simulated results almost 10 dB, this could be due the density of the lenses (90%), the fact the radiating patch don't have square shape and also due to an erroneous definition of the PLA dielectric values used for simulation.

4.6 Analysis of Results

In this section the simulated values and the measured results are resumed and analyzed. Also, a comparison between commercial and the 3D antennas are presented and discussed.

4.6.1 Performance analysis between the three antennas (simulated values)

In terms of gain, side lobe level, beamwidth, input impedance, bandwidth, return loss and antenna size obtained for each approach, it is shown in Table 4.3, the values obtained with simulation.

Parameter	**Without Lens**	**Extended hemispherical Lens**	**Spherical Lens**
Gain	6.14 dBi	16.97 dBi	16.35 dBi
Side Lobe Level	-	-10.9 dB	-16.5 dB
HPBW	107.7°	15.3°	21.5°
Input Impedance	$51.7 + j0.5\Omega$	$53 + j12.5\Omega$	$50.5 + j0.5\Omega$
Bandwidth	2.16 GHz	1.57 GHz	2 GHZ
Return Loss	-35.2 dB	-18.1 dB	-21.3 dB
Antenna Size	40x45x2.28 mm^3	40x45x57.28 mm^3	40x45x47.68 mm^3

Table 4.3: Performance analysis between the three antenna at 20 GHz

The extended hemispherical lens have provided the highest gain with 16.97 dBi, for the spherical lens, a gain of 16.35 dBi and the antenna without lens 6.14 dBi.

From the results in Table 4.3 its clear the increased directivity from the use of a single aperture coupled microstrip antenna compared to the application of a dielectric lens, with an increased of 10.83 dB for the extended hemispherical lens and 10.62 dB for the spherical lens.

It is clear, from the demonstrated values, that one can achieve very high gains by using dielectric lenses, although the bandwidth small decrease. It is comprehensible that there is going to be a limit to the possible radiation gain one can obtain, that will be bound by the decrease in radiation efficiency as the lens increases in size and the losses in the dielectric become more noticeable.

4.6.2 Comparison between simulation and measured results

On Table 4.4 it is shown the comparison between simulation and measured results in terms of gain, side lobe level, beamwidth, input impedance, bandwidth, return loss and antenna size obtained for each approach. It was not possible measure the gain of the antennas because i didn't have an reference antenna at 20 GHz.

Parameters	Extended hemispherical Lens		Spherical Lens	
	Simulated	*Measured*	*Simulated*	*Measured*
Gain	16.97 dBi	—	16.35 dBi	—
Side Lobe Level	-10.9 dB	-10 dB	-16.5 dB	-4.5 dB
HPBW	15.3°	28°	21.5°	31.5°
Input Impedance	$53 + j12.5\Omega$	$76 - j28\Omega$	$50.5 + j0.5\Omega$	$45 + j5\Omega$
Bandwidth	1.57 GHz	0.28 GHz	2 GHz	3.31 GHz
Return Loss	-18.1 dB	-10.22 dB	-21.3 dB	-21.41dB
Antenna Size	40x45x57.28 mm^3		40x45x47.68mm^3	

Table 4.4: Comparison between simulation and measured results of extended hemispherical and spherical lens at 20 GHz.

As already seen in previous sections the extended hemispherical lens presents a slight mismatch at 20 GHz, this leaves to a small bandwidth and return loss compared to the simulation, this could be to a misalignment of the gap with the patch, a few millimeters are critical at this frequency. However, the results of the radiation pattern, Figure 4.23 a), beamwidth and side lobe level have acceptable deviations.

Spherical lens antenna shows good matching at 20 GHz. In terms of return loss, bandwidth and input impedance this antenna have very acceptable measured values, better than extended hemispherical lens.

The largest difference between the measured and simulated values is in the side lobe level, Figure 4.23 b), the measured value is higher than the simulated, this may be due to the value used to the material density (PLA 90%) and the value of the permittivity used in the simulation.

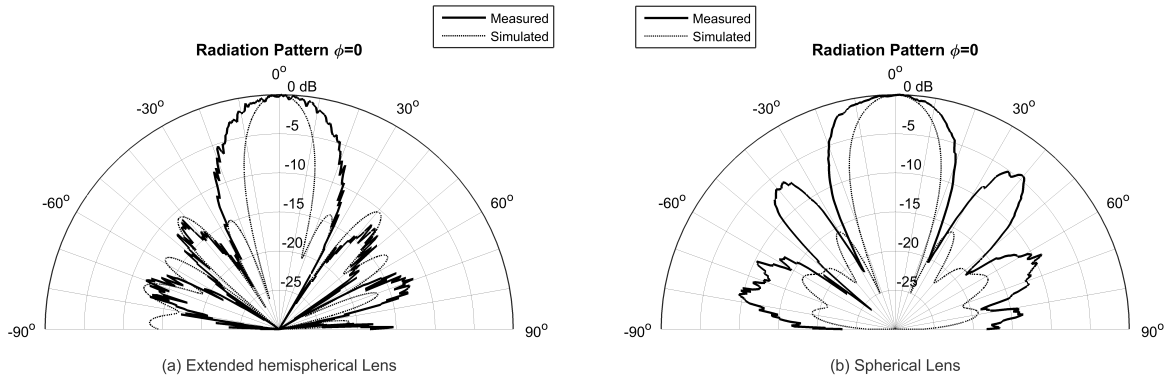

Figure 4.23: Simulated (Dashed) and Measured (Solid) radiation pattern for the 3D antennas

4.6.3 Comparison against commercial antennas

In this section the two 3D antennas, previously presented, are compared against three commercial antennas[34][35][36] that operates at the same frequency 20 GHz. The five antennas analyzed are shown in Figure 4.24.

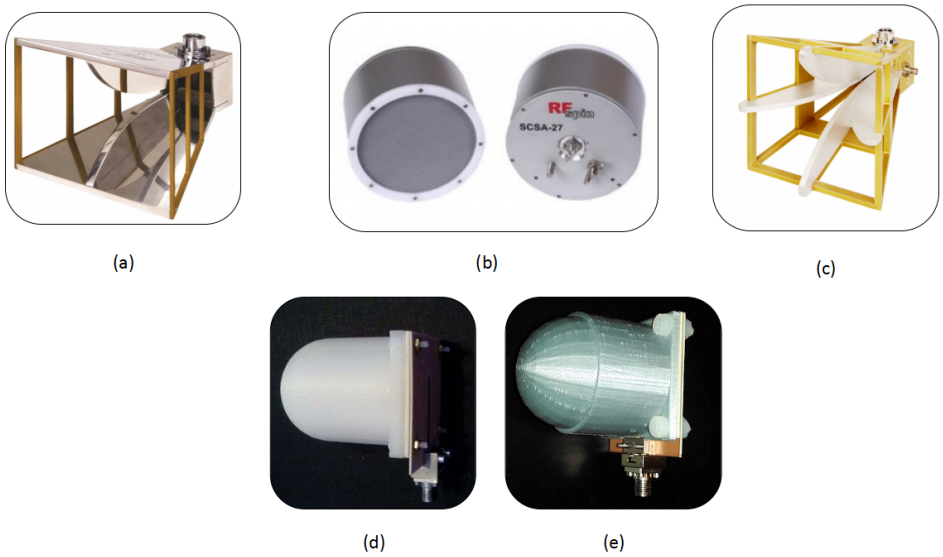

Figure 4.24: (a) DRH20 double ridged waveguide horn[34], (b) SCSA-27 spiral antenna[35], (c) QRH20E quad ridged horn[36], (d) Extended hemispherical lens fed by an aperture-coupled microstrip patch antenna, (e) Spherical lens fed by an aperture-coupled microstrip patch antenna.

Looking at Table 4.5 and Figure 4.25 it is possible to conclude that the 3D antennas are not behind the commercial ones in term of performance. The 3D antennas presents the highest gain and the smallest size. Relatively of adaptation (VSWR) at 20 GHz all antennas show good behavior, of the five, the antenna that have a less good adaptation is the extended hemispherical lens antenna for the reasons already mentioned previously. Like as expected the horns and 3D antennas show the sharpest beams in relation to the sphiral antenna. Analyzing Figure 4.25 is observed that the quad ridged horn presents lowest side lobe level, but the 3D antennas presents the smallest beamwidth.

Antenna	**Parameter**			
	Gain	*VSWR*	*HPBW*	Size
Double ridge waveguide horn	11 dBi	1.35	41°	104x122x78 mm^3
Spiral antenna	3 dBi	1.10	**114°	110x96x110 mm^3
Quad ridged horn	14 dBi	1.40	40°	101x101x132 mm^3
Extended hemispherical lens antenna	*16.97 dBi	1.89	28°	40x45x57.28 mm^3
Spherical lens antenna	*16.35 dBi	1.19	31.5°	40x45x47.68 mm^3

* Simulated value
** -10 dB beam width

Table 4.5: Performance analysis between 3D antennas against commercial antennas at 20 GHz

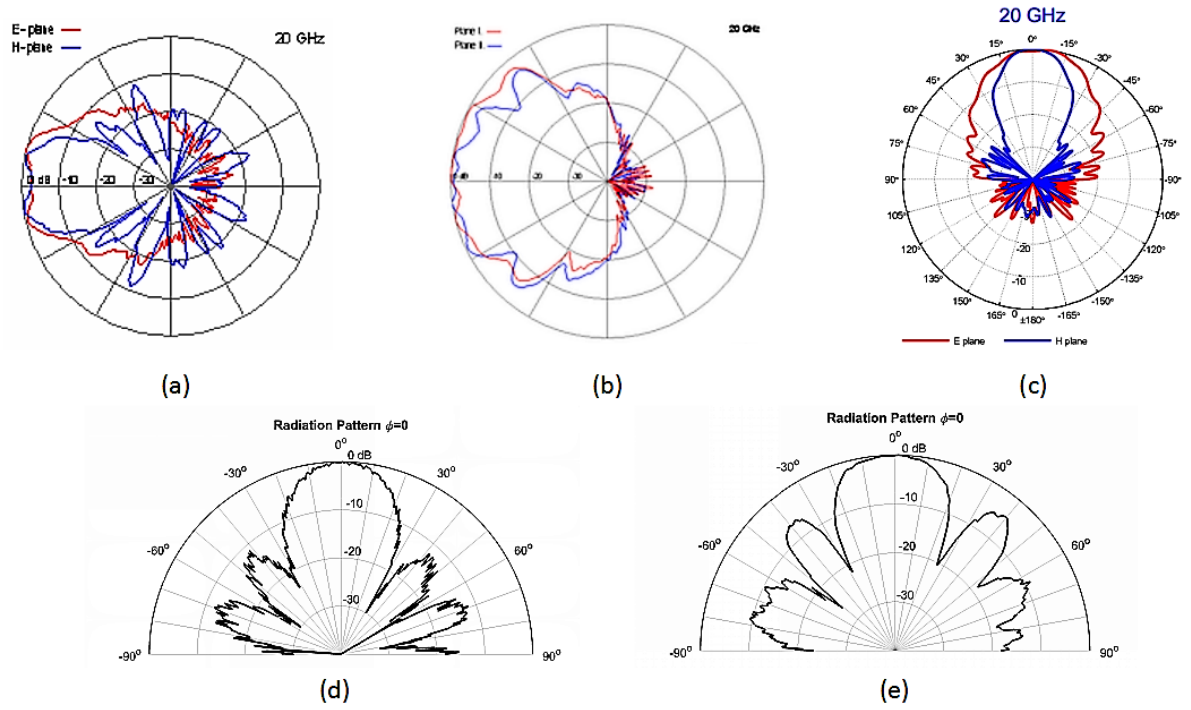

Figure 4.25: Radiation pattern comparison against commercial antennas at 20 GHz (a) DRH20 double ridged waveguide horn[34], (b) SCSA-27 spiral antenna[35], (c) QRH20E quad ridged horn[36], (d) Extended hemispherical lens fed by an aperture-coupled microstrip patch antenna, (e) Spherical lens fed by an aperture-coupled microstrip patch antenna.

Chapter 5

Conclusions

In this chapter, a general summary and the most important conclusions extracted from this work will be displayed and various research directions that can be followed, in order to improve the current system, will be pointed out. Besides this, the final section will present some final remarks on the importance of WPT.

5.1 General Analysis

The objective of WPT is to remove and eliminate all the power cables connected to the electronic utensils, but also to eliminate or at least reduce the charging needs of batteries in mobile devices. This technology is considered essential for the industry in several areas of expertise, including consumer electronics, automotive, and industrial control process.

The major drawback in these systems is their efficiency in energy transfer. The wavefronts of EM waves spread in space, dissipating the energy in all directions. To compensate wavefront spreading very high gain antennas are needed, such as antenna arrays of several elements, parabolic antennas, or lens antennas.

Dielectric lenses can be hard to fabricate, requiring molds that can be expensive. This cost can be significantly lowered and the fabrication process eased and speed up if we consider 3D printing technology.

In this dissertation, was presented the development of DLA's for transmission and harvesting of energy at the 20 GHz frequency for space applications; for example, to be used as a transmitting source to power up passive sensors in space.

3D printing was used to create lenses able to shape the radiation for a given antenna. Dielectric lens are used to shape wavefronts, much like reflectors, and can provide highly directive radiation patterns. Two different lenses were designed and developed using 3D printing, where a single slot coupled microstrip patch antenna was used as feeding source. The first was an extended hemispherical lens, wave front lens with compact size, which is the most simple wave-front shape lens design. Nevertheless, the overall gain of the spherical lens antenna was 16.97dBi, which is more than 10.87 dB improvement in gain compared to the single microstrip patch antenna radiation. In the second lens design, the radius of the lens base was kept the same, but the wavefront shape was changed from extended hemispherical to spherical lens, which resulted in an improved return loss and bandwidth in comparison to the extended hemispherical lens, with an overall gain of 16.35 dBi. However the side lobe level worsened in relation to the extended hemispherical lens.

5.2 Future Work

As any research work, some questions are answered, new questions and ideas arise. The following were those that seemed more interesting for further developments.

- Study the dielectric proprieties of the 3D printer material's at high frequencies, once new filaments are appear to the market (wood based, conductive and magnetic characteristics...). Knowledge of these properties it's crucial to get better results in simulation;
- Analyze the effect of printed material density on dielectric constant;
- Research new lens designs with multiple dielectric layers;
- Develop a WPT system, using this antenna models build a RF generator and a RF-to-DC that receives at 20 GHz;

5.3 Final Remarks

WPT is an emerging technology that is gaining increased visibility in recent years. Efficient WPT circuits, systems and strategies can address a large group of applications spanning from batteryless systems, battery-free sensors, passive RFID, near-field communications, and many others.

WPT is a fundamental enabling technology of the IoT concept, as well as machine-to-machine communications, since it minimizes the use of batteries and eliminates wired power connections.

The antennas proposed in this dissertation exhibit a high radiation gain, which is rather useful for, but is not limited to, applications to WPT. There is a compromise between the gain and the size and weight of the lens; therefore, depending on the gain levels one aims to reach, the viability of a lens antenna has to be carefully analysed. Therefore, DLA's can prove to be a solution for high-gain antenna and small size design for wireless energy transfer systems. This antennas also could be used for communications, there is nothing that limits them for this purpose.

Appendix A

3D Printing

Ink jet or laser printers produce most of today's documents or photographs. These create text or images by controlling the placement of ink or toner on the surface of a piece of paper. In a similar way, 3D printers manufacture objects by controlling the placement and adhesion of a "build material" in 3D space.

To 3D print an object, a digital model first needs to exist in a computer. This may be designed by hand using a computer aided design (CAD) application, or some other variety of 3D modeling software. Alternatively, a digital model may be created by scanning a real object with a 3D scanner, or perhaps by taking a scan of something and then tweaking it with software tools.

However the digital model is created, once it is ready to be fabricated some additional computer software needs to slice it up into a great many cross sectional layers only a fraction of a millimeter thick. These object layers can then be sent to a 3D printer that will print them out, one on top of the other, until they are built up into a complete 3D printed object.

Exactly how a 3D printer outputs an object one thin layer at a time depends on the particular technology on which it is based. There are more than a dozen viable 3D printing technologies. This said, almost all of them work in one of three basic ways.

Firstly, there are 3D printers that create objects by extruding a molten or otherwise semi-liquid material from a print head nozzle. Most commonly this involves extruding a continuous stream of hot thermoplastic that very rapidly sets after it has left the print head. There are even experimental 3D printers that output a computer-controlled flow of liquid concrete, and which may in the future allow whole buildings to be 3D printed.

A second category of 3D printer creates object layers by selectively solidifying a liquid known as a "photopolymer" – that hardens when exposed to a laser or other light source. Some such "photopolymerization" 3D printers build object layers within a tank of liquid photopolymer. Meanwhile others jet out a single layer of liquid and then use an ultraviolet light to set it solid before the next layer is printed. A few of the 3D printers that are based on the latter technology are able to mix and solidify many different photopolymers at the same time, so allowing them to print out multi-material objects made of parts with different material properties.

A final category of 3D printing hardware creates objects by selectively sticking together successive layers of a very fine powder. Such "granular materials binding" can be achieved either by jetting a liquid glue or "binder" onto each powder layer, or by fusing powder granules

together using a laser or other heat source. Already granular materials binding can be used to 3D print objects in a very wide range of materials. These include nylon, ceramics, wax, bronze, stainless steel, cobalt chrome and titanium.[37]

The printer used to print the lens on this dissertation was BEETHEFIRST [32], that use Fused Filament Fabrication (FFF) or Fused Deposition Modeling (FDM).

FFF is a method of rapid prototyping which works by laying down consecutive layers of material at high temperatures, allowing the adjacent layers to cool and bond together before the next layer is deposited, the process is presented in Figure A.1 b).

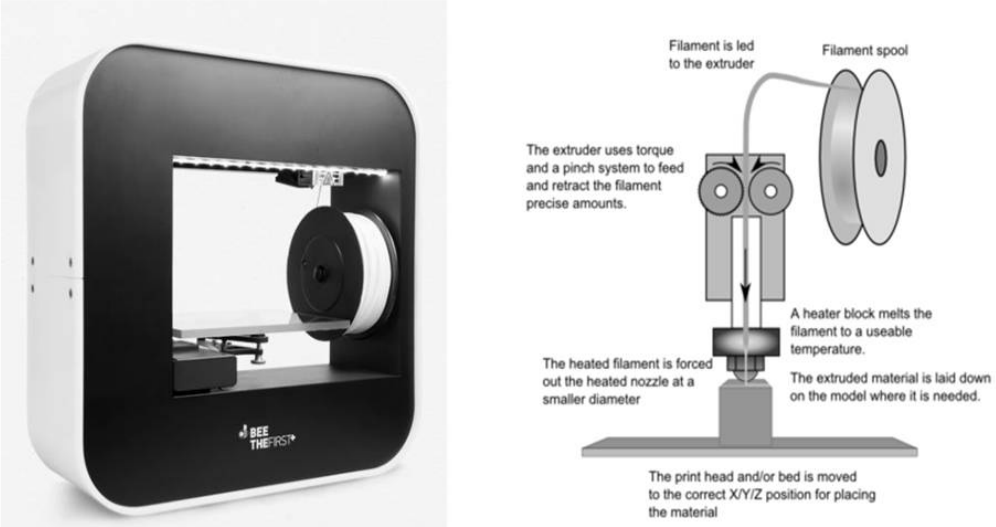

Figure A.1: (a) BEETHEFIRST 3D printer [32] (b) FFF method [38]

Appendix B

Article for the 10th Congress of the Portuguese Committee of URSI

3D Antenna for Wireless Power Transmission

Gonçalo Dias[1], Pedro Pinho[2], Ricardo Gonçalves[1], Nuno Carvalho[1]

[1]Instituto de Telecomunicações, Dep. de Eletrónica, Telecomunicações e Informática, Universidade de Aveiro, Portugal

[2]Instituto de Telecomunicações, ISEL, Portugal

***Abstract*—3D printers work with plastics materials, which are essentially dielectric. These can be used as radiating elements (dielectric resonators), as radiation handlers (lenses) or as a supporting base for applying conductive material to radiation (substrates). In this paper is explored the solution based on lenses, through the 3D printing technology. The design, simulation and build of an aperture coupled microstrip antenna with dielectric lens is presented in this paper. The antenna operates at 20 GHz. The lens is used to focus the beam of lower gain feed antenna to produced highly directive pattern with low side lobe levels**

***Index Terms*—3D antenna, 3D printing, Aperture coupled microstrip antenna with dielectric lens, Dielectric lens antennas, Wireless power transmission**

I. Introduction

The use of electronic devices has almost become a basic need given that the majority of jobs today depend on it to be executed. The great investment in research regarding the IoT is even pushing us to a greater dependency on self-sufficient electronic systems. The biggest disadvantage of current electronic devices comes from their dependence of external power connections or batteries in order to function. It is thus necessary to make these devices able to be powered on a more effective and versatile way. The development of WPT systems gets us closer to a truly wireless world, as it was imagined by several brilliant minds before us (Nikola Tesla, William C. Brown …). This will enable society a more comfortable use of electronics, be it from the integration of these mechanisms in implantable medical devices, the use of backscattering on sensors, easier charge of electronic devices, the power could be transmitted to the places where the wired transmission is not possible.

The 3D printing has seen a very strong growth in the last five years, especially since began to appear solutions of this kind of technology at much lower prices and for common user. It is possible to exploit the technology to create antennas with more complex shapes and in three dimensions quickly and much cheaper, that even here became only accessible to development teams of high budget projects, such as military or space. The design freedom associated with the three-dimensional structures can create complex geometries that produce very specific characteristics of radiation for very demanding applications. Today, it is possible to do this without big budgets.

The millimeter-wave and sub-millimeter frequency bands are very attractive for various modern indoor and outdoor applications. At these frequencies lenses become acceptable in size and weight for many applications. Lens antennas consist of two main parts: the feeding antenna that can be any other type of antenna (horns, dipoles, microstrip antennas, and even arrays of antenna elements) and lens that collimate incident divergent energy to prevent it from spreading in undesired directions. Integrated dielectric lens antennas (DLAs) [1], [2] are widely used in various communication, radar, and imaging systems in the millimeter (mm) and sub-mm wave bands. The key components of such antennas are dielectric lenses used for correction of radiation patterns of primary feeds - open waveguides or printed antennas.

Additionally, improvement of radiation efficiency is achieved due to a better matching (for the waveguide feeds) and a suppression of the surface waves (for the substrate mounted antennas). The common demands to novel DLAs are compact size and specific radiation patterns. A desired compromise between these two characteristics is not always easily achievable. Preliminary computer aided design (CAD) enables one to minimize the time and cost of a prototype development.

II. Aperture coupled microstrip antenna with dielectric lens

Aperture-coupled feed was originally proposed by Pozar [3]. This feed structure eliminates the asymmetry problems present in the microstrip line and coaxial probe. This type of feed consists of two substrates separated by a ground plane. On the bottom side of the lower substrate, there is a microstrip feed line which has the form of an open-circuit stub while the top side of the upper substrate contains the microstrip patch element.

The energy is electromagnetically coupled from the feed line to the patch through an aperture cut in the ground plane as shown in figure 1.

The main advantage of this configuration is that the feed network and the patch are well isolated from one another. In this way, no radiation from the feed network can interfere with the main radiation pattern since a ground plane separates the two mechanisms.

Back radiation from the feed network is an issue but it can be minimized by carefully sizing the slot. Another advantage of the aperture-coupling feed is that surface wave excitation can be better controlled by choosing different substrate

materials for the feed and radiating elements. The feed circuit layer can also be easily integrated with MMICs.

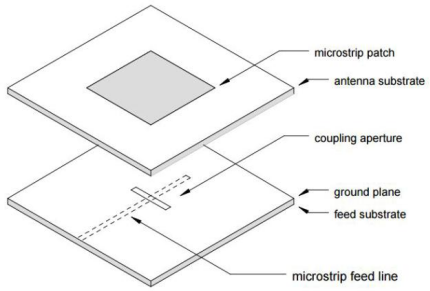

Fig. 1. Geometry of the basic aperture coupled microstrip antenna [3]

A. Design

In this paper is shown an aperture coupled microstrip antenna with a dielectric lens for WPT (Fig.2). The lens is used to focus the beam of lower gain feed antenna to produced highly directive pattern with low side lobe levels. The radiating microstrip patch element is etched on the top of the antenna substrate, and the microstrip feed line is etched on the bottom of the feed substrate.

The material used for the substrates was Isola Astra MT, which has 3 of permittivity. Lens is made of PLA that has been printed on a 3D printer. The antenna has designed for 20 GHz.

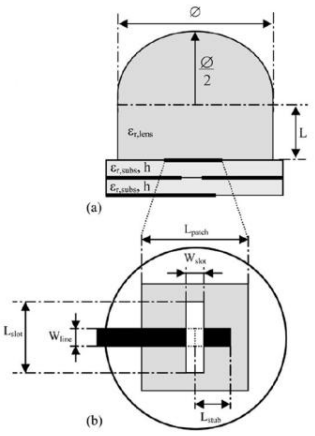

Fig. 2. Extended hemispherical lens fed by an aperture-coupled microstrip patch antenna (a) Cross-section view and (b) top view [4]

B. Simulation

For simulation purposes, the selected conductor was an infinitely thin copper padding with a conductivity of 5.8×10^7S/m and the lens was a permittivity of 1.8 with no losses.

The antenna has been modeled and optimized using the transient solver within CST MICROWAVE STUDIO®. Table 1 shows the antenna parameters.

TABLE I
ANTENNA DESIGN PARAMETERS

Parameter	Dimension (mm)
L_{patch}	3
W_{patch}	3
L_{slot}	3.5
W_{slot}	1.7
$L_{subPatch}$	40
$W_{subPatch}$	40
$L_{subLine}$	45
$W_{subLine}$	40
L_{line}	25
L_{stub}	5.5
W_{line}	1.93
h_{patch}	1.52
h_{feed}	0.76
L_{lens}	35
r_{lens}	20

Simulation results are used as the baseline antenna performance for comparison against all parametric adjustments. The center frequency, input impedance, VSWR, bandwidth and radiation patterns are determined and summarized below.

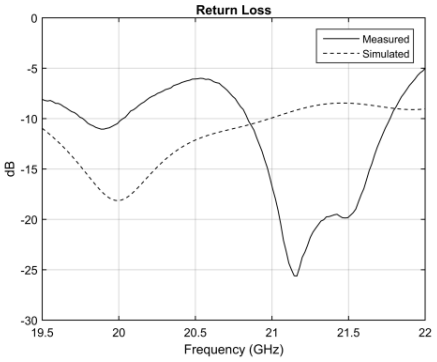

Fig. 3. Simulation and measurement of return loss

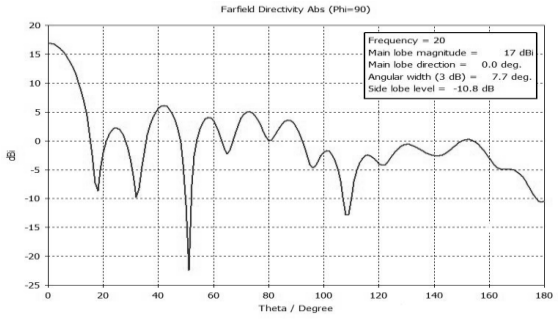

Fig. 4. Simulation result of farfield directivity

TABLE II
ANTENNA PARAMETERS @21.15GHZ

Input Impedance	55.4 + j 2.29 Ω
VSWR	1.11
Bandwidth	0.92 GHz
Radiation Efficiency	92.4%*

*simulated value at 20GHz

Figure 3 shows a good wideband behavior and return loss of the dielectric lens antenna. The "shift" of central frequency measured and the simulated, could be little misalignment of the slot with the patch and PLA dielectric value used for simulation. The resulting farfield can be seen in Figure 4. A high directivity of 17 dBi at the main beam and 92.4% radiation efficiency can be achieved with this dielectric lens antenna configuration.

C. 3D Printing

The printer used to print the lens was BEETHEFIRST, which use Fused Filament Fabrication (FFF) or Fused Deposition Modeling (FDM). [5]

FFF is a method of rapid prototyping which works by laying down consecutive layers of material at high temperatures, allowing the adjacent layers to cool and bond together before the next layer is deposited.

The software used to model the lens was OpenScad [6]. OpenSCAD is software for creating solid 3D CAD models. This isn't an interactive modeler, it's something like a 3D-compiler that reads in a script file that describes the object and renders the 3D model from this script file. This gives a full control over the modelling process and enables to easily change any step in the modelling process or make designs that are defined by configurable parameters.

Below is presented the lens with the antenna.

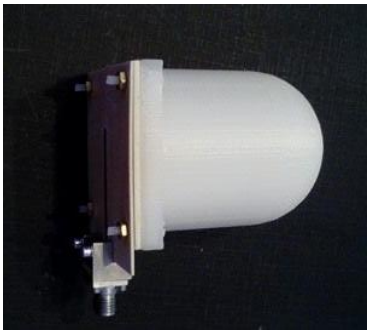

Fig. 6. 3D Antenna for Wireless Power Transmission

III. CONCLUSION

A design, simulation and build of a 3D antenna has been developed and presented with the intent of being used for wireless power transmission.

The next step is to make measurements of the antenna to confirm the simulation results and then connect to a power amplifier to proof of concept.

ACKNOWLEDGMENT

The authors acknowledge the Portuguese FCT/MCTES for financing the project UID/EEA/50008/2013.

REFERENCES

[1] A. V. Boriskin, R. Sauleau, and A. I. Nosich. 2-d analysis and synthesis of dielectric lens antennas with boundary integral equations. In Microwaves, Radar and Remote Sensing Symposium, 2008. MRRS 2008, pages 196–200, Sept 2008.

[2] T. Komljenovic and Z. Sipus. Dielectric lens antennas design at millimeter waves. In ELMAR, 2008. 50th International Symposium, volume 2, pages 621–624, Sept 2008.

[3] D. M. Pozar. Microstrip antenna aperture-coupled to a microstrip line. Electronics Letters, 21(2):49–50, January 1985.

[4] G. Godi, R. Sauleau, and D. Thouroude. Performance of reduced size substrate lens antennas for millimeter-wave communications. IEEE Transactions on Antennas and Propagation, 53(4):1278–1286, April 2005.

[5] C. Barnatt. 3D Printing: The Next Industrial Revolution. ExplainingTheFuture.com, 2013.

[6] OpenSCAD. 2016. OpenSCAD - The Programmers Solid 3D CAD Modeller. [ONLINE] Available at: http://www.openscad.org/. [Accessed 20 October 2016].

Appendix C

Article for the 2017 International Applied Computational Electromagnetics Society (ACES) Symposium

3D Antenna for Wireless Power Transmission

Aperture Coupled Microstrip Antenna with Dielectric Lens

Gonçalo Dias[1], Pedro Pinho[2], Ricardo Gonçalves[1], Nuno Carvalho[1]

[1]Instituto de Telecomunicações, Dep. de Eletrónica, Telecomunicações e Informática, Universidade de Aveiro, Portugal

[2]Instituto de Telecomunicações, ISEL, Portugal

Email: goncaloadias@ua.pt, ppinho@deetc.isel.pt, rgoncalves@av.it.pt, nbcarvalho@ua.pt

***Abstract*—Nowadays 3D printers are useful for the development and rapid prototyping of dielectric structures for radiation manipulation and support of antennas. This is possible since the materials used in this machines are essentially dielectric. These can be used as radiating elements (dielectric resonators), as radiation handlers (lenses) or as a supporting base for applying conductive material to radiation (substrates). In this paper we explore 3D printing technology to develop a lens antenna for wireless power transfer operating at 20 GHz. The design, simulation and measurement of an aperture coupled microstrip antenna with dielectric lens is presented and discussed. The lens is used to focus the beam of lower gain feed antenna to produce a highly directive pattern with low side lobe.**

Keywords—3D printing, Aperture coupled microstrip antenna, Dielectric lens antenna, Wireless power transmission.

I. INTRODUCTION

The great investment in research regarding the IoT is even pushing us to a greater dependency on self-sufficient electronic systems. The biggest disadvantage of current electronic devices comes from their dependence of external power connections or batteries in order to operate. It is thus necessary to make these devices able to be powered on a more effective and versatile way. The development of WPT (Wireless Power Transfer) systems gets us closer to a truly wireless world, as it was imagined by several brilliant minds before us (Nikola Tesla, William C. Brown …). This will enable society a more comfortable use of electronics, be it from the integration of these mechanisms in implantable medical devices, the use of backscattering on sensors, easier charge of electronic devices, the power could be transmitted to the places where the wired transmission is not possible.

Additive manufacturing, namely 3D printing, has seen a very strong growth in the last five years, especially since the first 3D printers for regular consumer use, at lower prices, started to appear in the market.

It is possible to exploit the technology to create antennas with more complex shapes and in three dimensions quickly and less expensive, that until here was only accessible to development teams with high budget projects, such as military or space. The design freedom associated with the three-dimensional structures allows the creation of complex geometries that produce very specific characteristics of radiation for very demanding applications.

Given the typical dimensions of lens antennas, and in order to operate within a constrained size, we opted to design and antenna for operation in the sub-millimeter frequency bands, namely at 20 GHz, which are very attractive for various modern indoor and outdoor applications. Lens antennas consist of two main parts: the feeding antenna can be of several types (horns, dipoles, microstrip antennas, and even arrays of antenna elements) and lens that collimate incident divergent energy to prevent it from spreading in undesired directions. Integrated dielectric lens antennas (DLAs) [1], [2] are widely used in various communication, radar, and imaging systems in the millimeter (mm) and sub-mm wave bands. The key components of such antennas are dielectric lenses used for correction of radiation patterns of primary feeds, open waveguides or printed antennas.

This paper is organized as follows, in section I a brief introduction to the lens antennas is presented. Section II describes the structure of the aperture coupled microstrip antenna and the dielectric lens dimensions. A comparison between simulation and measured results is also presented. Finally in section III we present the main conclusions.

II. APERTURE COUPLED MICROSTRIP ANTENNA WITH DIELECTRIC LENS

Aperture-coupled feed was originally proposed by Pozar [3]. This feed structure eliminates the asymmetry problems present in the microstrip line and coaxial probe. This type of feed consists of two substrates separated by a ground plane. On the bottom side of the lower substrate, there is a microstrip feed line which has the form of an open-circuit stub while the top side of the upper substrate contains the microstrip patch element.

The main advantage of this configuration is that the feed network and the patch are well isolated from one another. In this way, no radiation from the feed network can interfere with the main radiation pattern since a ground plane separates the two mechanisms.

A. Design

In this paper is shown an aperture coupled microstrip antenna with a dielectric lens for WPT (Fig.1). The lens is used to focus the beam of lower gain feed antenna to produced highly directive pattern with low side lobe levels. The radiating microstrip patch element is etched on the top of the antenna substrate, and the microstrip feed line is etched on the bottom of the feed substrate.

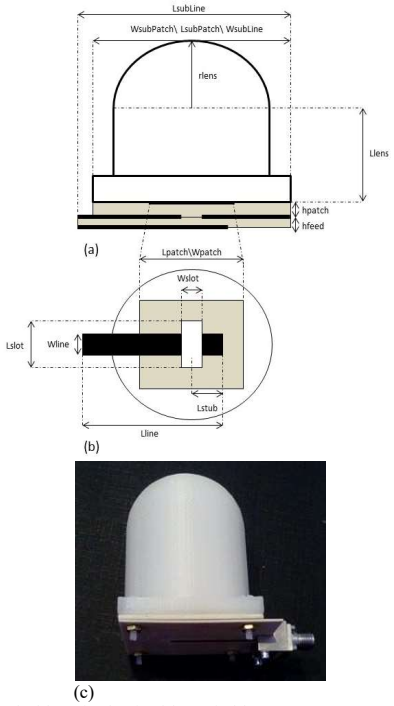

Fig. 1. Extended hemispherical lens fed by an aperture-coupled microstrip patch antenna (a) Cross-section view and (b) top view (c) photograph of the prototype.

The material used for both substrates was Isola Astra MT, which has a relative permittivity of 3.0 and a loss tangent of 0.0017. The lens is fabricated with PLA (Polyactic Acid) that has an estimated relative permittivity of 1.8 and a loss tangent of 0.01 [5]. The antenna has designed for 20 GHz.

B. Simulation

The antenna was modeled and optimized using the transient solver within CST MICROWAVE STUDIO®. The optimized physical parameters of the antenna are shown in Table 1.

TABLE I ANTENNA DESIGN PARAMETERS

Parameter	***Dimension (mm)***	***Parameter***	***Dimension (mm)***
Lpatch	3	Lens size	40x40x55
Wpatch	3	Lline	25
Lslot	3.5	Lstub	5.5
Wslot	1.7	Wline	1.93
LsubPatch	40	hpatch	1.52
WsubPatch	40	hfeed	0.76
LsubLine	45	Llens	35
WsubLine	40	rlens	20

C. Results

The simulated *versus* measured reflection coefficient obtained for the lens antenna is shown in Fig. 2. There is an observable shift in the measured resonant frequency that can be due to a misalignment of the line, slot and patch stacked structure, and also due to an erroneous definition of the PLA dielectric values used for simulation. The resulting farfield can be seen in Fig. 3 and 4. High directivity of 17 dBi at the main beam and 92.4% radiation efficiency can be achieved with this dielectric lens antenna configuration.

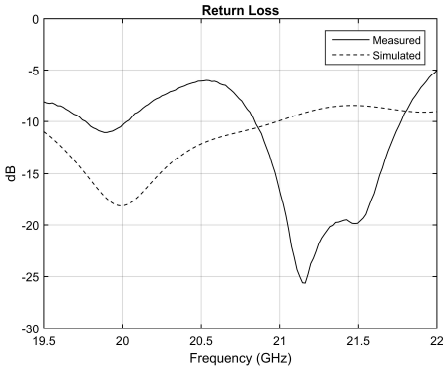

Fig. 2. Simulation and measurement of return loss

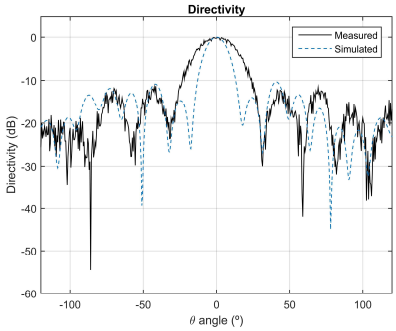

Fig. 3. Simulated and measured farfield directivity normalized

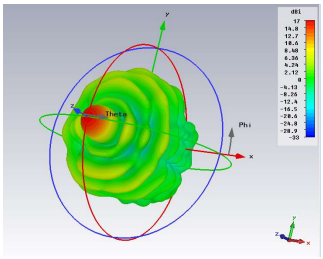

Fig. 4. Simulated 3D farfield directivity

III. CONCLUSION

A design, simulation and measurements of a 3D printed lens antenna has been presented with the intent of being used for wireless power transmission. The measurements match poorly to the simulation results and some improvements are required, namely in the correct definition of the lens material properties.

REFERENCES

[1] G. Eason, B. Noble, and I.N. Sneddon, "On certain integrals of Lipschitz-Hankel type involving products of Bessel functions," *Phil. Trans. Roy. Soc. London*, vol. A247, pp. 529-551, April 1955.

[2] J. Clerk Maxwell, A Treatise on Electricity and Magnetism, 3rd ed., vol. 2. *Oxford: Clarendon*, 1892, pp.68-73.

[3] D. M. Pozar. Microstrip antenna aperture-coupled to a microstrip line. *Electronics Lette*rs, 21(2):49–50, January 1985.

[4] G. Godi, R. Sauleau, and D. Thouroude. Performance of reduced size substrate lens antennas for millimeter-wave communications. *IEEE Transactions on Antennas and Propagation*, 53(4):1278–1286, April 2005

[5] R. Goncalves, R. Magueta, P. Pinho, N.B. Carvalho, Dissipation factor and permittivity estimation of dielectric substrates using a single microstrip line measurement, *Appl. Comput. Electromagn. Soc. J.* 31(2) (2016) 118–125.

References

[1] A. Carvalho, N. Carvalho, and P. Pinho. In *Wireless Power Transmission para Drones*, 2014.

[2] C. R. Valenta and G. D. Durgin. Harvesting wireless power: Survey of energy-harvester conversion efficiency in far-field, wireless power transfer systems. *IEEE Microwave Magazine*, 15(4):108–120, June 2014.

[3] H. Jabbar, Y. S. Song, and T. T. Jeong. Rf energy harvesting system and circuits for charging of mobile devices. *IEEE Transactions on Consumer Electronics*, 56(1):247–253, February 2010.

[4] A. J. Soares Boaventura, A. Collado, A. Georgiadis, and N. Borges Carvalho. Spatial power combining of multi-sine signals for wireless power transmission applications. *IEEE Transactions on Microwave Theory and Techniques*, 62(4):1022–1030, April 2014.

[5] A. Collado and A. Georgiadis. Improving wireless power transmission efficiency using chaotic waveforms. In *2012 IEEE/MTT-S International Microwave Symposium Digest*, pages 1–3, June 2012.

[6] Apostolos Georgiadis. Autonomous wireless sensors and rfid's: Energy harvesting material and circuit challenges. `http://www.laas.fr/files/RE-COM/121109GeorgiadisPres.pdf`, November 2012. Accessed: 2017-04-29.

[7] J.I. Agbinya. *Wireless Power Transfer*. The River Publishers Series in Communications. River Publishers, 2012.

[8] M.V. Acosta. *Advances in Energy Research*. Number vol. 8 in Advances in Energy Research. Nova Science Publishers, Incorporated, 2011.

[9] W. C. Brown. The history of power transmission by radio waves. *IEEE Transactions on Microwave Theory and Techniques*, 32(9):1230–1242, Sep 1984.

[10] André Kurs, Aristeidis Karalis, Robert Moffatt, J. D. Joannopoulos, Peter Fisher, and Marin Soljačić. Wireless power transfer via strongly coupled magnetic resonances. *Science*, 317(5834):83–86, 2007.

[11] N. Borges Carvalho, A. Georgiadis, A. Costanzo, H. Rogier, A. Collado, J. A. Garca, S. Lucyszyn, P. Mezzanotte, J. Kracek, D. Masotti, A. J. S. Boaventura, M. de las Nieves Ruz Lavn, M. Piuela, D. C. Yates, P. D. Mitcheson, M. Mazanek, and V. Pankrac. Wireless power transmission: R&d activities within europe. *IEEE Transactions on Microwave Theory and Techniques*, 62(4):1031–1045, April 2014.

[12] M. Piuela, P. D. Mitcheson, and S. Lucyszyn. Ambient rf energy harvesting in urban and semi-urban environments. *IEEE Transactions on Microwave Theory and Techniques*, 61(7):2715–2726, July 2013.

[13] R. Correia and N. Borges Carvalho. Quadrature amplitude backscatter modulator for passive wireless sensors. *10th Congress of the Portuguese Committee of URSI, Communications in security and emergency scenarios*, November 2016.

[14] R. Correia, A. Boaventura, and N. Borges Carvalho. Quadrature amplitude backscatter modulator for passive wireless sensors in iot applications. *IEEE Transactions on Microwave Theory and Techniques*, 65(4):1103–1110, April 2017.

[15] Ieee standard for definitions of terms for antennas. *IEEE Std 145-2013 (Revision of IEEE Std 145-1993)*, pages 1–50, March 2014.

[16] D.M. Pozar. *Microwave Engineering*. Wiley, 2004.

[17] Y. Huang and K. Boyle. *Antennas: From Theory to Practice*. Wiley, 2008.

[18] C.A. Balanis. *Antenna Theory: Analysis and Design*. Wiley, 2015.

[19] J Roelvink, S Trabelsi, and S O Nelson. Determining complex permittivity from propagation constant measurements with planar transmission lines. *Measurement Science and Technology*, 24(10):105001, 2013.

[20] Measuring the permittivity and permeability of lossy materials: solids, liquids, metals, building materials, and negative-index materials. *NIST Technical Note 1536*, 2005.

[21] Improved technique for determining complex permittivity with the transmission/reflection method. *IEEE Trans. Microw. Theory Tech.*, 38(8):1096, 1990.

[22] Janezic M D and Jargon J A. Complex permittivity determination from propagation constant measurements. *IEEE Microw. Guided Wave Lett.*, 9(2):76, 1999.

[23] J Roelvink, S Trabelsi, and S O Nelson. A planar transmission-line sensor for measuring the microwave permittivity of liquid and semisolid biological materials. *IEEE Trans. Instrum. Meas.*, 2013.

[24] A. V. Boriskin, R. Sauleau, and A. I. Nosich. 2-d analysis and synthesis of dielectric lens antennas with boundary integral equations. In *Microwaves, Radar and Remote Sensing Symposium, 2008. MRRS 2008*, pages 196–200, Sept 2008.

[25] T. Komljenovic and Z. Sipus. Dielectric lens antennas design at millimeter waves. In *ELMAR, 2008. 50th International Symposium*, volume 2, pages 621–624, Sept 2008.

[26] G. Godi, R. Sauleau, and D. Thouroude. Performance of reduced size substrate lens antennas for millimeter-wave communications. *IEEE Transactions on Antennas and Propagation*, 53(4):1278–1286, April 2005.

[27] D. M. Pozar. Microstrip antenna aperture-coupled to a microstripline. *Electronics Letters*, 21(2):49–50, January 1985.

[28] D. M. Pozar. A review of aperture coupled microstrip antennas: History, operation, development, and applications. Technical report, University of Massachusetts, May 1996.

[29] Isola astra mt datasheet. http://www.isola-group.com/wp-content/uploads/2016/09/Astra-MT77-Very-Low-loss-Laminate-Material-Data-Sheet-Isola.pdf. Accessed: 2016-09-06.

[30] R. Gonçalves, R. L. Magueta, P. Pinho, and N.B.C. Carvalho. Dissipation factor and permittivity estimation of dielectric substrates using a single microstrip line measurement. *Applied Computational Electromagnetics Society Journal*, 31(2):118–125, February 2016.

[31] Openscad. http://www.openscad.org/about.html. Accessed: 2017-02-12.

[32] Beethefirst specifications. https://beeverycreative.com/beethefirst-plus/. Accessed: 2016-09-07.

[33] L. Shafai. *Dielectric-Loaded Antennas*. John Wiley & Sons, Inc., 2001.

[34] RFspin. Double ridged waveguide horn model drh20 datasheet. http://www.rfspin.cz/uploads/files/cdec441762bd53775373920472559df73fd0b5cd/drh20.pdf. Accessed: 2017-06-05.

[35] RFspin. Spiral antenna model scsa-27 datasheet. http://www.rfspin.cz/uploads/files/89ce8cb941cd2b332027d7b3a85ab5cb0873e991/scsa-27.pdf. Accessed: 2017-06-05.

[36] RFspin. Quad ridged horn antenna model qrh20-e datasheet. http://www.rfspin.cz/uploads/files/bcf90cc93b450b1075bbe7ce5c5d0963bc989279/qrh20-e-datasheet-2013.pdf. Accessed: 2017-06-05.

[37] C. Barnatt. *3D Printing: The Next Industrial Revolution*. ExplainingTheFuture.com, 2013.

[38] Fff vs. sla vs. sls: 3d printing. http://www.sd3d.com/fff-vs-sla-vs-sls/. Accessed: 2016-09-07.